J Stat Phys (2014) 155:106–150
DOI 10.1007/s10955-014-0942-x

Accurate Expansions of Internal Energy and Specific Heat of Critical Two-Dimensional Ising Model with Free Boundaries

Xintian Wu · Ru Zheng · Nickolay Izmailian · Wenan Guo

Received: 2 September 2013 / Accepted: 29 January 2014 / Published online: 19 February 2014

Abstract The bond-propagation algorithm for the specific heat of the two dimensional Ising model is developed and that for the internal energy is completed. Using these algorithms, we study the critical internal energy and specific heat of the model on the square lattice and triangular lattice with free boundaries. Comparing with previous works (Phys Rev E 86:041149, 2012; Phys Rev E 87:022124, 2013), we reach much higher accuracy (10^{-28}) of the internal energy and specific heat, compared to the accuracy 10^{-11} of the internal energy and 10^{-9} of the specific heat reached in the previous works. This leads to much more accurate estimations of the edge and corner terms. The exact values of all edge and corner terms are therefore conjectured. The accurate forms of finite-size scaling for the internal energy and specific heat are determined for the rectangle-shaped square lattice with various aspect ratios and various shaped triangular lattice. For the rectangle-shaped square and triangular lattices and the triangle-shaped triangular lattice, there is no logarithmic correction terms of order higher than $1/S$, with S the area of the system. For the triangular lattice in rhombus, trapezoid and hexagonal shapes, there exist logarithmic correction terms of order higher than $1/S$ for the internal energy, and logarithmic correction terms of all orders for the specific heat.

Keywords Two dimensional Ising model · Free boundary · Bond propagation algorithm

X. Wu (✉) · R. Zheng · W. Guo
Department of Physics, Beijing Normal University, Beijing 100875, China
e-mail: wuxt@bnu.edu.cn

W. Guo
e-mail: waguo@bnu.edu.cn

N. Izmailian
Applied Mathematics Research Centre, Coventry University, Coventry CV1 5FB, UK

N. Izmailian
A.I. Alikhanyan National Science Laboratory, Alikhanian Br.2, 375036 Yerevan, Armenia
e-mail: izmail@yerphi.am

1 Introduction

The finite-size scaling theory, introduced by Fisher, finds extensive applications in the analysis of experimental, Monte Carlo, and transfer-matrix data, as well as in recent theoretical developments related to conformal invariance [1–4]. Exact solutions on the Ising model have been used to determine the form of finite-size scaling. Exact results of the model on finite sizes with various boundaries have been studied intensively [5–14]. Detailed knowledge has been obtained for the torus case [10,13], for helical boundary conditions [12], for Brascamp–Kunz boundary conditions [11,14] and for infinitely long cylinder[15].

However, the solution for the two-dimensional (2D) Ising model with free boundaries, i.e., with free edges and sharp corners, is difficult and not well studied up to now. Although there are Monte Carlo and transfer matrix studies on this problem [16,17], the accuracy, or the system sizes achieved, is not enough to extract the finite-size corrections. Meanwhile, for 2D critical systems, a huge amount of knowledge has been obtained by the application of the powerful techniques of integrability and conformal field theory (CFT) [3,4,18]. Cardy and Peschel [4] predicted that the next sub-dominant contribution to the free energy on a square comes from the corners, which is universal, and related to the central charge c in the continuum limit. Along this direction, boundary CFT has been studied intensively to treat critical systems with free boundaries in recent years [19,20]. It plays a fundamental role in our understanding of logarithmic conformal field theory [21,22], of the Kondo effect [23], of the physics of quantum impurities or the Fermi edge singularity [24], of local and global quenches in one-dimensional quantum systems [25–27], and, in the relationship between CFT and the Schramm Loewner Evolution formalism [28]. However, till now there is few studies on lattice model, say Ising model, with free boundary conditions to compare with the CFT results.

Recently there appear two successful approaches to solve the 2D Ising model with free boundaries. Vernier and Jacobsen [29] conjectured an exact analytic formula for the corner free energy of the Ising model on the square lattice based on the long series expansion. The asymptotic behavior upon approaching the critical temperature is shown to be consistent with CFT results. The other way is to use the bond propagation (BP) algorithm, which was developed for computing the partition function of the Ising model in two dimensions [30,31]. It is much faster than Monte Carlo simulation, and costs moderate memory comparing with the transfer matrix method. Very large system size can be reached. With this algorithm, the calculations have been carried out on square and triangular lattices with free boundaries [32, 33]. The results of free energy are surprisingly accurate to 10^{-26}. Fitting the assumed finite-size scaling formula to the data, the edge and corner terms were obtained very accurately. For example, from the corner term on the square lattice with rectangle shape [32], the central charge of Ising model was estimated as $c = 0.5 \pm 1 \times 10^{-10}$, compared with the CFT result $c = 0.5$ [4].

In the previous works [32,33], the critical internal energy and specific heat have also been studied by numerical differentiation of free energy [32,33]. However, the numerical differentiation process limits the accuracy to the order of 10^{-11} and 10^{-9}, respectively, which is much lower than that of the free energy. Therefore the authors could not determine the accurate expansion form for the internal energy and specific heat. For example, the authors could not extract the logarithmic correction at the third and fourth order in the expansions.

In present paper, we use the BP algorithms for internal energy and specific heat, rather than differentiation method, to study the critical internal energy and specific heat on the square and triangular lattices with free boundaries. We therefore obtained internal energy density and specific heat with accuracy much higher than those obtained in previous works. The

$Y-\Delta$ transformation in BP algorithm for internal energy was given by Loh et al. [31]. In this paper, we derive the BP series reduction for the internal energy, and make the algorithm completed. We also develop the BP algorithm for specific heat. The transformation in each step is exact. The numerical accuracy is limited by machine's precision, which is the round-off error 10^{-33} in the quadruple precision (note that there is 33 significant digits in quadruple precision format). The BP algorithm needs about N^3 steps to calculate the free energy of an $N \times N$ lattice (much faster than other numerical method). Therefore the total error is approximately $N^{3/2} \times 10^{-33}$. This estimation has been verified in the following way: We compared the results obtained using double precision, in which there are 16 effective decimal digits, and those using quadruple precision. Because the latter results are much more accurate than the formal, we can estimate the error in double precision results by taking the quadruple results as the exact results. We thus found that the error is about $N^{3/2} \times 10^{-16}$. In our calculation, the largest size reached is $N = 2,000$, the round-off error is less than 10^{-28}. Therefore using these algorithms, the accuracy of internal energy and specific heat reaches the same level as that of free energy, which is 10^{-28}. Fitting to these results, we obtain very accurate expansion of the internal energy and specific heat. The accurate expansions is helpful to the CFT and renormalization group (RG) study on this kind of problem [34].

For the square lattice, the rectangular shape with size $M \times N$ are studied. Five aspect ratios $\rho = M/N = 1, 2, 4, 8, 16$ are investigated. It is shown that the edge and corner internal energy are independent of aspect ratio, and there is no logarithmic correction term of order higher than $1/N^2$. For the triangular lattice, five shapes: triangular, rhomboid, trapezoid, hexagonal and rectangular, are studied. The logarithmic corrections terms $\ln N/N^4$, $\ln N/N^5, \ldots$ are found in the internal energy density, and logarithmic correction terms $\ln N/N^3$, $\ln N/N^4, \ldots$ are found in the specific heat for the rhomboid, trapezoid and hexagonal shapes, while there are no such terms for the triangular and rectangular shapes. Due to the high accuracy the exact values of all edge and corner terms are conjectured.

Our paper is organized as follows. Since this paper is very long, we first summarize our results in Sect. 2. In Sects. 3.1 and 3.2, we show the detail of fits on internal energy density and specific heat for the square lattice, respectively. In Sects. 4.1 and 4.2, we present results for the triangular lattice in five shapes respectively. We derive the BP algorithm for the specific heat in Sect. 5. Discussions and acknowledgements are given in Sect. 6.

2 Summary

In view of the length of this paper, we collect the principle results in this section .

We consider the partition function of the Ising model on a 2D lattice

$$Z = \sum_{\{\sigma\}} e^{-\beta H}, \tag{1}$$

where the Hamiltonian is given by,

$$\beta H = -\sum_{\langle ij \rangle} J_{ij} \sigma_i \sigma_j, \tag{2}$$

where $J_{ij} = \beta K_{ij}$ and $K_{ij} = K$ are the homogeneous couplings. The free energy density is defined as,

$$f = \frac{F}{S} = \frac{\ln Z}{S}, \tag{3}$$

where F, S are the total free energy and the number of spins (or the area of the system), respectively.

The internal energy density and specific heat density are defined as,

$$u = \frac{U}{S} = \frac{\partial f}{\partial \beta} = -\frac{1}{SZ}, \tag{4}$$

and

$$c = \frac{C}{S} = \beta^2 \frac{\partial^2 f}{\partial \beta^2}, \tag{5}$$

where U, C are the total internal energy and heat capacity. Note here the definition of internal energy is different from the ordinary one in the sign.

For the square lattice, we calculate the internal energy and specific heat at critical point $\beta_c = \frac{1}{2}\ln(1+\sqrt{2})$ with the BP algorithm. The calculations have been carried out for aspect ratios $\rho = M/N = 1, 2, 4, 8, 16$ on an $M \times N$ rectangular lattice.

We find that the critical internal energy can be expanded into

$$u = u_\infty + u_{\text{surf}} \frac{M \ln N + N \ln M}{S} + u_{\text{corn}} \frac{\ln S}{S} + \sum_{k=1}^{\infty} \frac{B_k}{S^{k/2}}. \tag{6}$$

Due to extraordinarily high accuracy, we can confirm the exact value for bulk internal energy u_∞ [5]

$$u_\infty^{\text{ex}} = \sqrt{2} \tag{7}$$

and we can conjecture the exact values of edge and corner terms

$$\begin{aligned} u_{\text{surf}}^{\text{ex}} &= -\frac{2}{\pi}; \\ u_{\text{corn}}^{\text{ex}} &= -\frac{\sqrt{2}}{\pi}. \end{aligned} \tag{8}$$

The detailed discussion on raw data and fitting procedure is presented in Sect. 3.1.

The critical specific heat can be expanded into

$$c = A_0^{\text{squ}} \ln N + D_0 + c_{\text{surf}} \frac{M \ln N + N \ln M}{S} + c_{\text{corn}} \frac{\ln S}{S} + \sum_{k=1}^{\infty} \frac{D_k}{S^{k/2}}. \tag{9}$$

We can confirm the exact value of A_0^{squ} [5]

$$A_0^{\text{ex,squ}} = \frac{2}{\pi}\left[\ln(1+\sqrt{2})\right]^2 \tag{10}$$

and conjecture that c_{surf} and c_{corn} are given by,

$$\begin{aligned} c_{\text{surf}}^{\text{ex}} &= \frac{3\sqrt{2}}{4} A_0^{\text{squ}}; \\ c_{\text{corn}}^{\text{ex}} &= \frac{3}{4} A_0^{\text{squ}}. \end{aligned} \tag{11}$$

The corresponding detailed discussion on raw data and fitting is presented in Sect. 3.2.

For the triangular lattice, we have studied five shapes: triangle, rhombus, trapezoid, hexagon and rectangle, as shown in Fig. 1. Using the BP algorithms for the internal energy and specific heat, we obtain the critical energy density and specific heat for the five shapes at the exact critical point $\beta_c = \frac{1}{4}\ln(3) = 0.274653072167\ldots$.

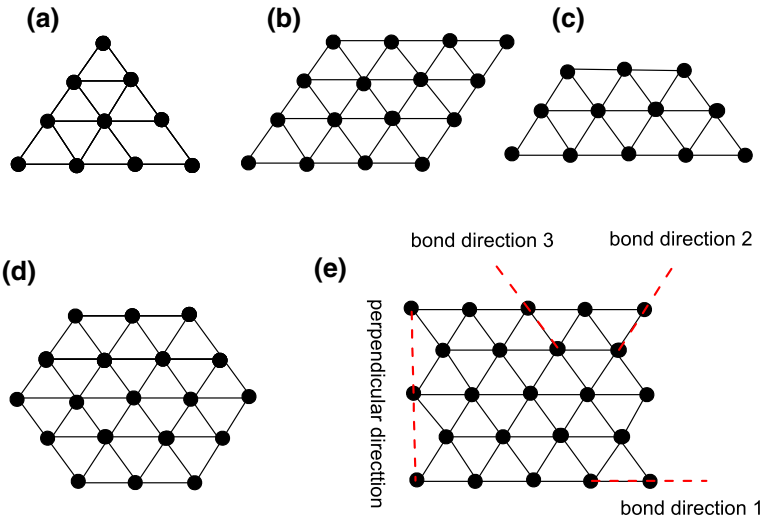

Fig. 1 **a** The *triangle-shaped* triangular lattice with $N = 4$. **b** The *rhombus-shaped* lattice with $N = 4$. **c** The trapezoid-shaped lattice with $N = 3$. **d** The *hexagon-shaped* lattice with $N = 3$. **e** The it rectangle-shaped lattice with $N = 5$. In the numerical calculation, we set the numbers of spins at the *bottom* and *top* and the number of layers be equal to an odd number. Three bond directions and the perpendicular direction are shown (see text)

We find that the expansion of the critical internal energy is given by

$$u = u_\infty + u_{\rm surf}\frac{p(N)\ln N}{S} + \frac{u_1}{S^{1/2}} + \frac{u_{\rm corn}\ln N + u_2}{S} + \frac{u_3}{S^{3/2}} + \sum_{k=4}^{\infty}\frac{u_k + u_{lk}\ln N}{S^{k/2}}. \tag{12}$$

The linear size N of a finite lattice is defined as the number of spins at edges in the triangle, rhombus and hexagon cases, of which the length of edges are equal. For the trapezoid shape, the lengths of the three shorter edges are required to be equal and N is the number of spins at the shorter edges. For the rectangle shape, N is defined as the number of spins at the bottom edge, and the number of layers is also required to be N. Moreover we set N be an odd number. $p(N)$ is the perimeter, which equals to $3N, 4N, 5N-1, 6N, (2+\sqrt{3})N$ for the triangle, rhombus, trapezoid, hexagon and rectangle, respectively. The area S, i.e. the number of spins on the lattice, is given by $S = N(N+1)/2, N^2, N(3N-1)/2, 3N^2-3N+1, N^2-(N-1)/2$ for the triangle, rhombus, trapezoid, hexagon and rectangle shaped system, respectively. We denote the surface internal energy per unit length of the edge along one bond direction by $u_{\rm surf}^{\parallel}$, and that perpendicular to that direction by $u_{\rm surf}^{\perp}$. Under the assumption that $u_{\rm corn}$ is the sum of the corner's contributions, we get each corner's contribution. For example, we assume $u_{\rm corn} = 6u_{\rm corn}^{(2\pi/3)}$ for the hexagonal shape. We confirmed the exact result of bulk term [7]

$$u_\infty^{\rm ex} = 2; \tag{13}$$

and conjectured the edge and corner terms

$$
\begin{aligned}
u_{\text{surf}}^{\text{ex},\parallel} &= u_{\text{surf}}^{\text{ex},\perp} = -\frac{\sqrt{3}}{\pi};\\
u_{\text{corn}}^{\text{ex},(\pi/3)} &= -\frac{\sqrt{3}}{\pi};\\
u_{\text{corn}}^{\text{ex},(\pi/2)} &= \frac{1}{4\pi}(2\sqrt{3}-3);\\
u_{\text{corn}}^{\text{ex},(2\pi/3)} &= \frac{1}{\sqrt{3}\pi}.
\end{aligned}
\tag{14}
$$

About the rectangular shape, some further explanations are necessary. Note that the formula of perimeter and area for rectangular shape is only valid for such shape shown in Fig. 1e, in which the numbers of spin at the top and bottom equal to an odd number N, and the number of layers also equals to N. In the numerical calculation, we only study such lattices. One could change the rectangle by removing one row from the bottom and adding one row to the top. The new rectangle has the same aspect ratio as the original, but the the formula for the area must be modified.

The expansion of the critical specific heat be

$$
\begin{aligned}
c = A_0^{\text{tri}} \ln N + c_0 + c_{\text{surf}} \frac{p(N)\ln N}{S} + \frac{c_1}{S^{1/2}}\\
+ \frac{c_{\text{corn}} \ln N + c_2}{S} + \sum_{k=3} \frac{c_k + c_{lk} \ln N}{S^{k/2}}.
\end{aligned}
\tag{15}
$$

We denote the surface specific heat per unit length of the edge along one bond direction by $c_{\text{surf}}^{\parallel}$, and that perpendicular to that direction by $c_{\text{surf}}^{\perp}$. Under the assumption that c_{corn} is the sum of the corner's contributions, we get each corner's contribution. We confirmed the exact result of the leading term [7]

$$
A_0^{\text{ex,tri}} = \frac{3\sqrt{3}}{4\pi}(\ln 3)^2;
\tag{16}
$$

and we conjectured the edge terms and corner terms

$$
\begin{aligned}
c_{\text{surf}}^{ex,\parallel} &= \frac{A_0^{\text{ex,tri}}}{3};\\
c_{\text{surf}}^{ex,\perp} &= \frac{A_0^{\text{ex,tri}}}{6}(3-\sqrt{3});\\
c_{\text{corn}}^{ex,(\pi/3)} &= \frac{A_0^{\text{ex,tri}}}{2};\\
c_{\text{corn}}^{ex,(\pi/2)} &= \frac{A_0^{\text{ex,tri}}}{24}(3\sqrt{3}-7);\\
c_{\text{corn}}^{ex,(2\pi/3)} &= -\frac{A_0^{\text{ex,tri}}}{9}.
\end{aligned}
\tag{17}
$$

The details of the triangular lattice are given in Sect. 4.

3 Critical Internal Energy and Specific Heat on the Square Lattice with Rectangular Shape

We calculate the internal energy and specific heat at critical point $\beta_c = \frac{1}{2}\ln(1+\sqrt{2})$ with the BP algorithms. The calculations have been carried out for aspect ratios $\rho = M/N = 1, 2, 4, 8, 16$ on an $M \times N$ rectangular lattice.

In reference [32], the critical internal energy density on the square lattice with rectangle shape has been studied. The internal energy was obtained by numerical differentiating the free energy, which was calculated by BP algorithm for the partition function. Although the accuracy of free energy is the machine precision, the accuracy of internal energy can only reach $\sim 10^{-11}$. The fitting parameters for the higher order terms for the internal energy are not accurate enough. In the best fits, the authors can only fit the data up to the term $1/N^4$. More importantly, the accurate form of the fitting formula can not be determined. For example, the authors can not determine whether there exists a $\ln N/N^4$ term or not. Using the BP algorithm for the internal energy, the accuracy of internal energy reaches 10^{-26}, so we can expand the internal energy to much higher order terms. More accurate expansion form can be determined.

The number of data points of internal energy and specific heat are 120, 117, 117, 103, 92 for $\rho = 1, 2, 4, 8, 16$, respectively. The fitting interval of sizes is $30 \le N \le 2{,}000$ for $\rho = 1, 2$. It is $30 \le N \le 1{,}800$ for $\rho = 4$. They are $30 \le N \le 1{,}350$ and $30 \le N \le 1{,}000$ for $\rho = 8, 16$, respectively. Some selected raw data are listed in Appendix 1 for the convenience of future readers to check.

3.1 Internal Energy Density

We fit the data of critical internal energy with the formula given by

$$u = u_\infty + u_{\rm surf}\frac{M\ln N + N\ln M}{S} + u_{\rm corn}\frac{\ln S}{S} + \sum_{k=1}^{k_{max}} \frac{B_k}{S^{k/2}}, \tag{18}$$

with k from 1 to 15.

In Table 1, we show the fitted $u_\infty, u_{\rm surf}, u_{\rm corn}$. We list 31 digits for these results for the convenience of future readers who may want to check other functional forms for the size and shape dependence of the free energy. The estimated errors are also listed.

The bulk value u_∞ is known from the exact solution of Onsager [5]. It is given by

$$u_\infty^{\rm ex} = \sqrt{2} = 1.41421356237309504880168872420\ldots \tag{19}$$

The leading correction is due to the edges. In the exact result of Au-Yang and Fisher [9] on the strip with two free edges, the edges' correction is obtained as $-\frac{2}{\pi}\ln N/N$. It is natural to conjecture that, on the rectangle with four free edges, the edge correction is given by $-\frac{2}{\pi}(M\ln N + N\ln M)/(MN)$ with the coefficient $u_{\rm surf}^{\rm ex}$. Therefore the exact value of $u_{\rm surf}$ should be

$$u_{\rm surf}^{\rm ex} = -\frac{2}{\pi} = -0.63661977236758134307553505 3\ldots. \tag{20}$$

Following the convention in the critical free energy, we write the coefficient of $(\ln S)/S$ as $u_{\rm corn}$. From the fitted $u_{\rm corn}$ in Table 1, we conjecture that it equals to

$$u_{\rm corn}^{\rm ex} = -\frac{\sqrt{2}}{\pi} = -0.45015815807855303477759 95\ldots, \tag{21}$$

Table 1 The fitted u_∞, edge, corner free energy density in Eq. (18) for $\rho = 1, 2, 4, 8, 16$

ρ	u_∞	Δu_∞
1	0.14142135623730950488016887328 59D+01	0.2D−25
2	0.14142135623730950488016887267 73D+01	0.2D−25
4	0.14142135623730950488016887256 65D+01	0.2D−26
8	0.14142135623730950488016887269 26D+01	0.5D−26
16	0.14142135623730950488016887285 23D+01	0.2D−25
ρ	u_{surf}	Δu_{surf}
1	−0.63661977236758134307556947931 65D+00	0.6D−22
2	−0.63661977236758134307554850525 05D+00	0.9D−22
4	−0.63661977236758134307554462509 86D+00	0.1D−22
8	−0.63661977236758134307555123432 37D+00	0.3D−22
16	−0.63661977236758134307555947263 51D+00	0.9D−22
ρ	u_{corn}	Δu_{corn}
1	−0.45015815807855303483248090000 12D+00	0.9D−19
2	−0.45015815807855303480952077071 04D+00	0.2D−18
4	−0.45015815807855303481640240412 97D+00	0.4D−19
8	−0.45015815807855303487838109436 25D+00	0.2D−18
16	−0.45015815807855303503981199229 32D+00	0.8D−18

which is independent of aspect ratio ρ, hence geometry independent. The accuracy of this result reaches 10^{-19}, much higher than that in the previous work [32].

The other fitting parameters B_k are listed in Tables 2, 3, 4, 5, 6.

Since we conjectured out the exact values of surface and corner terms, we redo the fitting for the data with the conjectured exact values in the following way

$$u = \sqrt{2} - \frac{2}{\pi}\frac{M\ln N + N\ln M}{S} - \frac{\sqrt{2}}{\pi}\frac{\ln S}{S} + \sum_{k=1}^{k_{max}} \frac{B'_k}{S^{k/2}}, \tag{22}$$

with k from 1 to 15. The refitted parameters are shown in Tables 2, 3, 4, 5, 6. Comparing the original fit and the latter fit with conjectured exact values of bulk, surface and corner terms, one can see that the accuracy of all other parameters increases, especially for the lower order terms.

To characterize the accuracy of our fits, we define the maximal deviation

$$\delta_{max} = Max|y_i - y_i^{fit}|, \tag{23}$$

where y_i is the numerical data and y_i^{fit} is the value given by the fitting formula. We choose the maximum of the deviations from the data to the fitted ones to represent our fitting quality. We expand the internal energy to as high order as possible to make the δ_{max} as small as possible. In our fittings for the internal energy density, it has $\delta_{max} < 10^{-28}, 10^{-28}, 10^{-29}, 10^{-28}, 10^{-29}$ for $\rho = 1, 2, 4, 8, 16$ respectively. In the refittings with the conjectured bulk, edge and corner terms, we have $\delta_{max} < 10^{-28}, 10^{-28}, 10^{-29}, 10^{-29}, 10^{-29}$ for $\rho = 1, 2, 4, 8, 16$ respectively.

The term $B_1/S^{1/2}$ in fact scales as $1/N$. In the infinitely long strip limit, the coefficient of $1/N$ is known as $-\frac{2}{\pi}(\frac{7}{2}\ln 2 + \gamma - \frac{\pi}{4} - \ln\pi) \approx -0.683158$ [9]. As we can see in Tables 2, 3, 4,

Table 2 The fitted parameters B_k in Eq. (18) and the refitted parameters B'_k in Eq. (22) for $\rho = 1$

k	B_k	ΔB_k
1	−0.12136266920589298903556271999 95D+00	0.1D−20
2	−0.98613268253549279209568369430 95D+00	0.1D−17
3	−0.29552917347572967991830617956 34D+00	0.7D−16
4	−0.61687177276949016112438354355 54D−01	0.1D−13
5	0.20822475285719555000270904765 91D+00	0.1D−11
6	−0.53427354272445566922826855061 64D+00	0.2D−09
7	0.12217885239241647624039360363 25D+01	0.2D−07
8	−0.29573046308801160376540923991 77D+01	0.1D−05
9	0.75202477036782960288220652433 22D+01	0.6D−04
10	−0.22356385593614800878672852495 87D+02	0.3D−02
11	0.74055865522721538025622213403 81D+02	0.8D−01
12	−0.27916574203452544590132435594 71D+03	0.2D+01
13	0.10584143975613943594898061145 16D+04	0.2D+02
14	−0.35587955313575389466707964488 50D+04	0.2D+03
15	0.63005568586950660981356857985 11D+04	0.9D+03
k	B'_k	$\Delta B'_k$
1	−0.12136266920589298903616575291 26D+00	0.2D−24
2	−0.98613268253549279275737812908 59D+00	0.4D−21
3	−0.29552917347572963375945230598 17D+00	0.4D−18
4	−0.61687177276956698714444921168 86D−01	0.2D−15
5	0.20822475285841913506985525423 40D+00	0.6D−13
6	−0.53427354288115888197034132041 09D+00	0.1D−10
7	0.12217885393820442687275572262 64D+01	0.1D−08
8	−0.29573057886828293612640944500 59D+01	0.1D−06
9	0.75203129965947303993110517517 44D+01	0.9D−05
10	−0.22359128274290613178973716525 20D+02	0.4D−03
11	0.74140145200146979675386628160 05D+02	0.2D−01
12	−0.28100197313247214721163417905 97D+03	0.4D+00
13	0.10852397913564963317382428623 97D+04	0.6D+01
14	−0.37942113332336938565933205037 98D+04	0.6D+02
15	0.72379253372577101108626177500 20D+04	0.2D+03

5, 6, $B_1/\sqrt{\rho} = -0.12136\ldots, -0.18287\ldots, -0.32269\ldots, -0.44776\ldots, -0.53778\ldots$ for $\rho = 1, 2, 4, 8, 16$ respectively. It approaches the limit $-0.683158\ldots$ as ρ increases. We have tried other forms of formula to fit the critical internal energy. The logarithmic correction in higher order terms such as $\ln S/S^{3/2}$, $\ln S/S^2, \ldots$ are excluded clearly since their coefficients are extremely small if these terms are taken into account. Moreover the standard deviations of the fits with these terms are much larger than those without them.

Why do we fit the data in the interval of size beginning from $N = 30$? Because the fitting formula Eq. (18) is only expanded to 15th order, the truncation error should be proportional to N^{-16}, which are about 6.0×10^{-12}, 10^{-16}, 10^{-19} and 2.0×10^{-21} for $N = 5, 10, 15, 20$, respectively. These values are much larger than the accumulated round-off error in the BP algorithm, which is about 10^{-28}. If the data with $N = 5$ is included and the fitting accuracy reaches 10^{-28}, we need to expand the internal energy density at least to 30th order. However

Table 3 The fitted parameters B_k in Eq. (18) and the refitted parameters B'_k in Eq. (22) for $\rho = 2$

k	B_k	ΔB_k
1	−0.25861915103289093588725004802 51D+00	0.2D−20
2	−0.11259958889214527703275806610 76D+01	0.2D−17
3	−0.98611731959497394622438594750 92D−01	0.2D−15
4	−0.49305681377833214949228960641 56D+00	0.4D−13
5	0.11009631445392196872429707871 65D+01	0.8D−11
6	−0.26716642441785971539784524652 44D+01	0.1D−08
7	0.71329869538257958510314889051 76D+01	0.2D−06
8	−0.22053907590818531623171466666 03D+02	0.2D−04
9	0.75432393655280878903445710321 60D+02	0.1D−02
10	−0.29609518599003443157528819827 08D+03	0.9D−01
11	0.12912056735745769569113177473 73D+04	0.4D+01
12	−0.63742212024172290827496920900 70D+04	0.1D+03
13	0.32382850516010602011437651766 48D+05	0.2D+04
14	−0.14835527423103236146949084256 07D+06	0.3D+05
15	0.37452049526339844209334795156 93D+06	0.2D+06
k	B'_k	$\Delta B'_k$
1	−0.25861915103289093588750630697 73D+00	0.3D−24
2	−0.11259958889214527707341653542 21D+01	0.9D−21
3	−0.98611731959497356860332763095 79D−01	0.1D−17
4	−0.49305681377834100286364658535 95D+00	0.8D−15
5	0.11009631445412079801158649064 50D+01	0.3D−12
6	−0.26716642445379143927333783983 39D+01	0.9D−10
7	0.71329870038661127926320132012 05D+01	0.2D−07
8	−0.22053912884154052928755853225 76D+02	0.2D−05
9	0.75432815350913403933483630970 85D+02	0.2D−03
10	−0.29612021430020045651418972266 72D+03	0.1D−01
11	0.12922925183760856825429622412 67D+04	0.7D+00
12	−0.64076877740808378962015747051 67D+04	0.2D+02
13	0.33073900659539486205475060709 88D+05	0.6D+03
14	−0.15692784641895115187814083955 52D+06	0.8D+04
15	0.42277351868637281516252892816 15D+06	0.5D+05

this would induce another severe drawback. For the data of large size, say $N = 100$, the higher order terms, say higher than 15 order, in the expansion become smaller than the data accuracy 10^{-28}. Then they play no role in determining the fitting parameters of higher order terms. As we know, we are concerning with the asymptotic behavior of large size system, so the data with larger size should be more important. Therefore we discard the data of sizes less than $N = 30$ in the fitting.

Of course we can predict the data with sizes less than 30 with our fitting formula. This would provide one additional diagnostic on our choice of functional form. In Table 29 in Appendix 2, we present the internal energy density obtained by the fitting formula Eq. (18) with size $N = 5, 10, 15, 20$. Some further discussions are given in the Appendix.

Table 4 The fitted parameters B_k in Eq. (18) and the refitted parameters B'_k in Eq. (22) for $\rho = 4$

k	B_k	ΔB_k
1	−0.64539799424371914759615778370 99D+00	0.3D−21
2	−0.17143235174874349016718672418 49D+01	0.6D−18
3	0.84584180209496352278562906089 91D+00	0.6D−16
4	−0.28216522214525089692650222289 59D+01	0.2D−13
5	0.74044703371922294205221381660 53D+01	0.5D−11
6	−0.23050143086840052569663681341 36D+02	0.1D−08
7	0.82026388795779110419534951527 97D+02	0.2D−06
8	−0.33846072307824420141943270524 46D+03	0.3D−04
9	0.15667326105500024258540388364 24D+04	0.4D−02
10	−0.82606458368793610863191221728 54D+04	0.3D+00
11	0.48468981790908880169878430070 33D+05	0.2D+02
12	−0.31893414656962985428130315445 58D+06	0.8D+03
13	0.21832147923104176779512311058 13D+07	0.2D+05
14	−0.13606059029575068022441769175 49D+08	0.4D+06
15	0.48958759153990436773981698241 25D+08	0.3D+07
k	B'_k	$\Delta B'_k$
1	−0.64539799424371914759637457829 22D+00	0.4D−25
2	−0.17143235174874349021943333530 17D+01	0.2D−21
3	0.84584180209496358847711708076 79D+00	0.3D−18
4	−0.28216522214525308538798626140 22D+01	0.3D−15
5	0.74044703371991883143207865483 59D+01	0.2D−12
6	−0.23050143088617658748079739001 11D+02	0.7D−10
7	0.82026389145442999358735852574 94D+02	0.2D−07
8	−0.33846077530692537074278532779 41D+03	0.4D−05
9	0.15667384854506989493310369327 86D+04	0.5D−03
10	−0.82611381866984409181152796235 78D+04	0.5D−01
11	0.48499173677322927975236863683 18D+05	0.3D+01
12	−0.32024713769741624154346371259 13D+06	0.2D+03
13	0.22215093189493428085318999848 28D+07	0.5D+04
14	−0.14277119774952871299358155543 88D+08	0.1D+06
15	0.54295087667844917106253675222 40D+08	0.8D+06

3.2 Critical Specific Heat

The data of the critical specific heat are fitted according to the formula

$$c = A_0^{\mathrm{squ}} \ln N + D_0 + c_{\mathrm{surf}} \frac{M \ln N + N \ln M}{S} + c_{\mathrm{corn}} \frac{\ln S}{S} + \sum_{k=1}^{\infty} \frac{D_k}{S^{k/2}}, \tag{24}$$

with k from 1 to 15. The leading term $A_0^{\mathrm{squ}} \ln N$ is known from Onsager's exact result [5], which reads

$$A_0^{\mathrm{ex,squ}} = \frac{2}{\pi}[\ln(1+\sqrt{2})]^2 = 0.49453858953231911786500 31\ldots. \tag{25}$$

Table 5 The fitted parameters B_k in Eq. (18) and the refitted parameters B'_k in Eq. (22) for $\rho = 8$

k	B_k	ΔB_k
1	−0.12664842818618753617095532074 53D+01	0.8D−21
2	−0.32029302923645063785749791999 75D+01	0.2D−17
3	0.39841408844276596402479068645 18D+01	0.3D−15
4	−0.12980684800740433480397286029 65D+02	0.1D−12
5	0.45243158669378144103909069575 40D+02	0.4D−10
6	−0.19122225001156809098586190223 94D+03	0.1D−07
7	0.93578663781277965900220567619 93D+03	0.4D−05
8	−0.53047693409214920698615515421 11D+04	0.7D−03
9	0.33894317930691439002642673419 05D+05	0.1D+00
10	−0.24506462855154729673018918489 87D+06	0.1D+02
11	0.19685913474235194499120948854 51D+07	0.1D+04
12	−0.17554573481029432246052601396 42D+08	0.6D+05
13	0.16327021896397177845575807319 34D+09	0.2D+07
14	−0.13848880822950505433210531212 72D+10	0.6D+08
15	0.70251400413706251555658226277 64D+10	0.6D+09
k	B'_k	$\Delta B'_k$
1	−0.12664842818618753617100079568 24D+01	0.9D−25
2	−0.32029302923645063799743859925 28D+01	0.5D−21
3	0.39841408844276598549710644527 11D+01	0.1D−17
4	−0.12980684800740526451013414601 48D+02	0.2D−14
5	0.45243158669417458391004544732 76D+02	0.1D−11
6	−0.19122225002513757001034453944 72D+03	0.7D−09
7	0.93578664145947667222398822576 63D+03	0.2D−06
8	−0.53047700909308632188742401494 39D+04	0.6D−04
9	0.33894434747128714297959031633 30D+05	0.1D−01
10	−0.24507824030687848995842206303 28D+06	0.2D+01
11	0.19697555043756323822812349757 40D+07	0.2D+03
12	−0.17625350499124552134265833185 82D+08	0.1D+05
13	0.16616141209976482423023065015 70D+09	0.5D+06
14	−0.14559514588333464465397580505 65D+10	0.1D+08
15	0.78186985430125695303503057903 16D+10	0.2D+09

Among the five aspect ratios, the worst fit gives $A_0^{\mathrm{squ}} \approx 0.4945385895323191178650 3(9)$, which agrees with the exact result in the accuracy 10^{-22}. Other fitted parameters are listed in Table 7.

The constant c_0 increases with the aspect ratio. For the strip case it is known that $c_0(\rho = \infty) = -(\frac{7}{2}\ln 2 + \gamma - 14\xi(3)/\pi^2 - \frac{\pi}{4} - \ln\pi) \approx -0.3125538$ [9]. It is $-0.57078\ldots$, $-0.44276\ldots$, $-0.37766\ldots$, $-0.34510\ldots$ and $-0.32883\ldots$ for $\rho = 1, 2, 4, 8$ and 16, respectively, see Table 7. As the aspect ratio increases, c_0 approaches the limit $c_0(\rho = \infty)$. However we have not obtained an analytical expression for the dependence of c_0 on ρ.

The term $(M \ln N + N \ln M)/S$ is the next order correction. From the fit of c_{corn}, listed in Table 7, one can see that it is independent of ρ. We conjecture that its exact value is given by

Table 6 The fitted parameters B_k in Eq. (18) and the refitted parameters B'_k in Eq. (22) for $\rho = 16$

k	B_k	ΔB_k
1	−0.21515386777211102868062072101 18D+01	0.3D−20
2	−0.64921696989147234508003921109 03D+01	0.1D−16
3	0.13519911055294311742169774485 70D+02	0.2D−14
4	−0.55310890032304717111064442049 67D+02	0.9D−12
5	0.26542942332867922220678823151 66D+03	0.5D−09
6	−0.15570622048732792810788376069 77D+04	0.2D−06
7	0.10631139059385850326822505356 66D+05	0.7D−04
8	−0.83991477285100966982691229761 69D+05	0.2D−01
9	0.74932770469542172119683335506 62D+06	0.4D+01
10	−0.75336372122898041199745577925 98D+07	0.6D+03
11	0.83998685876637548059388849119 53D+08	0.7D+05
12	−0.10319513272820961674527718296 63D+10	0.6D+07
13	0.13218288804435244819812035615 66D+11	0.3D+09
14	−0.15426834932095564052882210764 69D+12	0.1D+11
15	0.11030363439121508841692641771 80D+13	0.2D+12
k	B'_k	$\Delta B'_k$
1	−0.21515386777211102868071064868 67D+01	0.2D−24
2	−0.64921696989147234545792109477 12D+01	0.2D−20
3	0.13519911055294312474067174581 59D+02	0.5D−17
4	−0.55310890032305137912807290228 59D+02	0.9D−14
5	0.26542942332891827673096361348 54D+03	0.1D−10
6	−0.15570622049851889994068292471 92D+04	0.7D−08
7	0.10631139100487933264739217151 14D+05	0.4D−05
8	−0.83991488907406657093401005182 58D+05	0.1D−02
9	0.74933020527675252224563888888 91D+06	0.3D+00
10	−0.75340412172114120038304042399 93D+07	0.7D+02
11	0.84046738507904563308828428330 51D+08	0.9D+04
12	−0.10360239855219145413260435097 30D+10	0.8D+06
13	0.13450667409448985187163259947 98D+11	0.5D+08
14	−0.16225933820367465115552641275 79D+12	0.2D+10
15	0.12280486770615152139127894342 11D+13	0.3D+11

$$c_{\text{surf}}^{\text{ex}} = \frac{3\sqrt{2}}{4} A_0^{\text{ex,squ}} = 0.5245373853251001248\ldots. \tag{26}$$

In the previous work it is estimated as $c_{\text{surf}} = 0.524529(3)$ [32]. Note that this term is absent in the torus case [8] and not mentioned in the infinitely long strip case [9], but exists in the cylinder case with Brascamp–Kunz boundary conditions [14,11].

The corner term c_{corn} seems also independent of aspect ratio ρ and its exact value is conjectured as

$$c_{\text{corn}}^{\text{ex}} = \frac{3}{4} A_0^{\text{ex,squ}} = 0.370903942149239338\ldots. \tag{27}$$

Table 7 The fitted A_0^{squ}, edge, corner specific in Eq. (24)

ρ	A_0^{squ}	ΔA_0^{squ}
1	0.49453858953231911786500326073 44D+00	0.2D−23
2	0.49453858953231911786500319112 29D+00	0.2D−25
4	0.49453858953231911786500318135 43D+00	0.3D−24
8	0.49453858953231911786500318618 24D+00	0.7D−24
16	0.49453858953231911786500301755 07D+00	0.3D−24
ρ	c_{surf}	Δc_{surf}
1	0.52453738532510012474465858747 09D+00	0.7D−20
2	0.52453738532510012474442634549 09D+00	0.1D−21
4	0.52453738532510012474438576056 11D+00	0.2D−20
8	0.52453738532510012474441074383 00D+00	0.4D−20
16	0.52453738532510012474366580869 47D+00	0.1D−20
ρ	c_{corn}	Δc_{corn}
1	0.37090394214923933865292890873 32D+00	0.5D−17
2	0.37090394214923933851519154171 43D+00	0.1D−18
4	0.37090394214923933851329992203 51D+00	0.3D−17
8	0.37090394214923933865229543891 91D+00	0.1D−16
16	0.37090394214923933568791043652 97D+00	0.7D−17

The other parameters $D_1, D_2, \cdots$ are fitted and listed in Tables 8, 9, 10, 11, 12. We have tried other forms of formula to fit the specific heat. The logarithmic correction in higher order terms such as $\ln S/S^{3/2}$, $\ln S/S^2, \ldots$ are excluded clearly since their coefficients are extremely small if these terms are taken into account. Moreover the standard deviations of the fits with these terms are much larger than those without them.

We also redo the fitting for the data of the critical specific heat with the exact value of A_0^{squ}, c_{surf}, c_{corn}

$$c = A_0^{\text{ex,squ}} \ln N + D_0 + c_{\text{surf}}^{\text{ex}} \frac{M \ln N + N \ln M}{S} + c_{\text{corn}}^{\text{ex}} \frac{\ln S}{S} + \sum_{k=1}^{\infty} \frac{D_k'}{S^{k/2}}, \tag{28}$$

with k from 1 to 15 and $A_0^{\text{ex,squ}}$, $c_{\text{surf}}^{\text{ex}}$, $c_{\text{corn}}^{\text{ex}}$ are given by Eq. (25), (26), and (27), respectively. The refitted parameters are given in Tables 8, 9, 10, 11, 12.

In our fits for the specific heat, the maximal deviation defined in Eq. (23) is $\delta_{max} < 10^{-27}, 10^{-29}, 10^{-28}, 10^{-28}, 10^{-29}$ for $\rho = 1, 2, 4, 8, 16$, respectively. In the refittings with the conjectured bulk, edge and corner terms, we have $\delta_{max} < 10^{-27}, 10^{-28}, 10^{-28}, 10^{-29}, 10^{-29}$ for $\rho = 1, 2, 4, 8, 16$ respectively.

4 Critical Internal Energy and Specific Heat on the Triangular Lattice with Free Boundaries

For the triangular lattice, we have studied five shapes: triangle, rhombus, trapezoid, hexagon and rectangle, as shown in Fig. 1. Using the BP algorithms for the internal energy and specific

Table 8 The fitted parameters D_k in Eq. (24) and the refitted parameters D'_k in Eq. (28) for $\rho = 1$

k	D_k	ΔD_k
0	−0.57078620770669870300691327537 05D+00	0.2D−22
1	−0.69883722953369806645389328285 56D+00	0.1D−18
2	0.11264987839373629446845791759 35D+01	0.6D−16
3	0.15426462287060853968692577371 67D+00	0.3D−14
4	0.72511922531849583993655603244 02D−01	0.3D−12
5	−0.29189844962294713919469840586 50D+00	0.4D−10
6	0.64864576413019236681849922273 64D+00	0.4D−08
7	−0.14600601257269032194533755982 52D+01	0.4D−06
8	0.34126437118820325378611953185 06D+01	0.2D−04
9	−0.96171524512134631181084641410 48D+01	0.1D−02
10	0.31052034012222294122577442154 36D+02	0.5D−01
11	−0.12081917203434801743671678554 21D+03	0.1D+01
12	0.51298110660444311721784540884 03D+03	0.3D+02
13	−0.23768999398012901551568955663 71D+04	0.4D+03
14	0.94767527887412353370648149968 99D+04	0.3D+04
15	−0.25843584335267218172790210772 80D+05	0.1D+05
k	D'_k	$\Delta D'_k$
0	−0.57078620770669870300691236910 26D+00	0.4D−26
1	−0.69883722953369806644885620633 75D+00	0.1D−22
2	0.11264987839373629474927518601 16D+01	0.2D−19
3	0.15426462287060839542650076029 92D+00	0.1D−16
4	0.72511922531868288575863688586 90D−01	0.4D−14
5	−0.29189844962546166114845746989 87D+00	0.1D−11
6	0.64864576441566099355799632255 37D+00	0.2D−09
7	−0.14600601514904780484030690154 58D+01	0.2D−07
8	0.34126455152630522600621823671 61D+01	0.2D−05
9	−0.96172489096739088152701827556 26D+01	0.1D−03
10	0.31055918098810137513999465927 68D+02	0.7D−02
11	−0.12093448743428405052426787547 41D+03	0.2D+00
12	0.51542298221238731209076146621 81D+03	0.5D+01
13	−0.24117311107007423865043064346 85D+04	0.8D+02
14	0.97762911779490692595652009560 16D+04	0.8D+03
15	−0.27015717887493987392097741977 98D+05	0.3D+04

heat, we obtain the critical energy density and specific heat for the five shapes at the exact critical point $\beta_c = \frac{1}{4}\ln(3) = 0.274653072167\ldots$. The linear size N of a finite lattice is defined as the numbers of spin on the edges in the triangle, rhombus and hexagon cases, of which the length of edges are equal. For the trapezoid shape, the lengths of the three shorter edges are required to be equal and N is the length of the shorter edges. For the rectangle, N is defined as the number of spin at the bottom edge, and the number of layers is also required to be N. However, the actual geometrical vertical length is $N\sqrt{3}/2$. According to the finite-size

Table 9 The fitted parameters D_k in Eq. (24) and the refitted parameters D'_k in Eq. (28) for $\rho = 2$

k	D_k	ΔD_k
0	−0.44276299836893728512626738654191D+00	0.2D−24
1	−0.62635173101060511781350097869 47D+00	0.2D−20
2	0.12893849732698279106756588832 58D+01	0.1D−17
3	−0.98775256694470042443935289946 98D−01	0.8D−16
4	0.50733070796002769136499360812 97D+00	0.1D−13
5	−0.11746661848937230952994128769 94D+01	0.2D−11
6	0.27774794718432127501938850405 43D+01	0.3D−09
7	−0.75933645314508497284920827246 04D+01	0.4D−07
8	0.23102771499938509801029956823 81D+02	0.4D−05
9	−0.82884839009540987008965260693 58D+02	0.3D−03
10	0.34014515847833663638758451477 31D+03	0.2D−01
11	−0.16867710616783532785505738773 60D+04	0.6D+00
12	0.94339200328283549781407868717 26D+04	0.2D+02
13	−0.59042817228822841150718099641 93D+05	0.4D+03
14	0.32537907737353457692509914252 11D+06	0.4D+04
15	−0.12377117123837662532689628202 43D+07	0.2D+05
k	D'_k	$\Delta D'_k$
0	−0.44276299836893728512627368129 01D+00	0.4D−27
1	−0.62635173101060511781190036610 46D+00	0.2D−23
2	0.12893849732698279120540689952 58D+01	0.3D−20
3	−0.98775256694470139737925308672 59D−01	0.3D−17
4	0.50733070796004600826692831385 26D+00	0.2D−14
5	−0.11746661848972642334917214172 50D+01	0.7D−12
6	0.27774794724177714817997909111 91D+01	0.2D−09
7	−0.75933646052716292588093086810 91D+01	0.3D−07
8	0.23102778838238519700136262316 16D+02	0.4D−05
9	−0.82885395569818398917208105521 81D+02	0.3D−03
10	0.34017690484132207298055356535 65D+03	0.2D−01
11	−0.16881053374405957242957757702 06D+04	0.1D+01
12	0.94739007807980251509384727622 86D+04	0.3D+02
13	−0.59849573611901355491141982831 25D+05	0.8D+03
14	0.33519186475037835181586134390 59D+06	0.1D+05
15	−0.12920152758049578806431701449 14D+07	0.6D+05

scaling [1], the system size should be the actual geometrical length, not the number of layers. Therefore the aspect ratio of the rectangle, we consider here, is $\sqrt{3}/2$ rather than 1.

The number of data points of internal energy and specific heat are 123, 148, 153, 193, 194 for triangular, rectangular rhomboid, trapezoid and hexagonal shape, respectively. The size range is $30 \leq N \leq 2{,}000$ for the triangular shape. For the rectangular shape, it is $31 \leq N \leq 1{,}999$. They are $32 \leq N \leq 2{,}000$, $32 \leq N \leq 1{,}950$, and $32 \leq N \leq 1{,}240$, for the rhomboid; trapezoid and hexagonal shape, respectively. Some selected raw data are listed in Appendix 1 for the convenience of future readers to check.

Table 10 The fitted parameters D_k in Eq. (24) and the refitted parameters D'_k in Eq. (28) for $\rho = 4$

k	D_k	ΔD_k
0	−0.37766121531044869122617062810 76D+00	0.3D−23
1	−0.44573067371552735647648268352 47D+00	0.3D−19
2	0.19047721206063732912432634504 24D+01	0.3D−16
3	−0.11553518282057856624908857813 06D+01	0.3D−14
4	0.28507669966409254461327573267 39D+01	0.7D−12
5	−0.76013113339118775868603157888 69D+01	0.2D−09
6	0.23008895112228663836475299342 86D+02	0.3D−07
7	−0.80890380716782174694362060670 58D+02	0.5D−05
8	0.32126972252776668261938499970 61D+03	0.7D−03
9	−0.14813604070424934814253530801 31D+04	0.7D−01
10	0.78069372904585053121028421730 54D+04	0.6D+01
11	−0.49206222258868815129512856018 24D+05	0.3D+03
12	0.35619613234916650747913488311 78D+06	0.1D+05
13	−0.29424924058271962109815572941 44D+07	0.4D+06
14	0.22054321975031754684138829730 57D+08	0.6D+07
15	−0.11571623941392267258439430289 85D+09	0.5D+08
k	D'_k	$\Delta D'_k$
0	−0.37766121531044869122617054559 68D+00	0.5D−27
1	−0.44573067371552735647539636890 57D+00	0.3D−23
2	0.19047721206063732926844000163 10D+01	0.8D−20
3	−0.11553518282057858001058425486 02D+01	0.1D−16
4	0.28507669966409622669847970036 11D+01	0.8D−14
5	−0.76013113339219352861371255701 17D+01	0.4D−11
6	0.23008895114528244753349016267 59D+02	0.1D−08
7	−0.80890381132703125109285202207 46D+02	0.3D−06
8	0.32126978071846008221049111396 99D+03	0.6D−04
9	−0.14813666195320857822006431879 95D+04	0.8D−02
10	0.78074362675344923425412895116 82D+04	0.7D+00
11	−0.49235763291589123657982578985 93D+05	0.5D+02
12	0.35744347426730140457806634695 18D+06	0.2D+04
13	−0.29779723982326553580280174734 67D+07	0.7D+05
14	0.22662847817631068447337388325 45D+08	0.1D+07
15	−0.12046615216078931405706785167 48D+09	0.1D+08

4.1 Critical Internal Energy Density

We fit the data of critical internal energy with the formula given by

$$u = u_\infty + u_{\text{surf}} \frac{p(N) \ln N}{S} + \frac{u_1}{S^{1/2}} + \frac{u_{\text{corn}} \ln N + u_2}{S} + \frac{u_3}{S^{3/2}} + \sum_{k=4}^{\infty} \frac{u_k + u_{lk} \ln N}{S^{k/2}}, \quad (29)$$

Table 11 The fitted parameters D_k in Eq. (24) and the refitted parameters D'_k in Eq. (28) for $\rho = 8$

k	D_k	ΔD_k
0	−0.345107484255949676000133509814 9D+00	0.7D−23
1	−0.190599347476723075814404423735 0D+00	0.9D−19
2	0.339319896411104663836139495069 0D+01	0.1D−15
3	−0.450409008759588366526384528397 3D+01	0.1D−13
4	0.130585957467102389760482187684 7D+02	0.4D−11
5	−0.457549616239733079779033492753 9D+02	0.1D−08
6	0.187261432796818622815574012649 5D+03	0.4D−06
7	−0.888191501663727112400044704559 8D+03	0.9D−04
8	0.476228890480164012284129972667 0D+04	0.2D−01
9	−0.291058306351702897826465932775 9D+05	0.2D+01
10	0.200777242956950398151069407166 8D+06	0.2D+03
11	−0.161376229210894161696962271526 3D+07	0.2D+05
12	0.148713905104610230647501500575 2D+08	0.1D+07
13	−0.157392991384474750161271542692 0D+09	0.4D+08
14	0.156276835794280804316215689664 0D+10	0.1D+10
15	−0.110769966369940255402689796327 9D+11	0.1D+11
k	D'_k	$\Delta D'_k$
0	−0.345107484255949676000133379091 4D+00	0.8D−28
1	−0.190599347476723075812436641144 7D+00	0.7D−24
2	0.339319896411104664164592148272 7D+01	0.2D−20
3	−0.450409008759588403829838069208 0D+01	0.4D−17
4	0.130585957467103648499283305766 2D+02	0.4D−14
5	−0.457549616240177240603934008477 2D+02	0.3D−11
6	0.187261432810185183570329529515 0D+03	0.1D−08
7	−0.888191504891645358434262921021 3D+03	0.5D−06
8	0.476228951439748351165143569419 0D+04	0.1D−03
9	−0.291059192211736102095770496945 3D+05	0.2D−01
10	0.200786990810292464823243043742 3D+06	0.3D+01
11	−0.161455697631363714603108610785 4D+07	0.2D+03
12	0.149177834878193962754439365046 5D+08	0.2D+05
13	−0.159223456492470381911743428093 2D+09	0.7D+06
14	0.160643181438240207777032418519 4D+10	0.2D+08
15	−0.115520381739855393001741013584 1D+11	0.2D+09

where $p(N)$ is the perimeter, which equals to $3N, 4N, 5N-1, 6N, (2+\sqrt{3})N$ for the triangle, rhombus, trapezoid, hexagon and rectangle, respectively. The area S, i.e. the number of spins on the lattice, is given by $S = N(N+1)/2$, N^2, $N(3N-1)/2$, $3N^2-3N+1$, $N^2-(N-1)/2$ for the triangle, rhombus, trapezoid, hexagon and rectangle shaped system, respectively. This expansion is different from that for the triangular lattice with periodic boundary conditions [13], in which there's no surface, corner terms, logarithmic corrections, and only even k presents. In addition there are logarithmic correction in higher order terms

Table 12 The fitted parameters D_k in Eq. (24) and the refitted parameters D'_k in Eq. (28) for $\rho = 16$

k	D_k	ΔD_k
0	−0.32883061871232049899139905320 93D+00	0.3D−23
1	0.13230380377457662135031976458 30D+00	0.5D−19
2	0.66271437033732753234897713424 37D+01	0.9D−16
3	−0.14487827869486893960095693221 10D+02	0.1D−13
4	0.55545449916104030018849053526 34D+02	0.4D−11
5	−0.26662260251049611637805063301 99D+03	0.2D−08
6	0.15108538336641212983548681064 52D +04	0.7D−06
7	−0.98961174791216038807542073719 07D+04	0.2D−03
8	0.73172451222088136772509012604 81D+05	0.5D−01
9	−0.60865937878816414682197821793 31D+06	0.9D+01
10	0.56405606300351988091798778544 65D+07	0.1D+04
11	−0.59201061584813782313048164385 16D+08	0.1D+06
12	0.70137558271348826218284295160 36D+09	0.1D+08
13	−0.94819880741664040203546916538 94D+10	0.6D+09
14	0.12461804276614917990723683671 32D+12	0.2D+11
15	−0.11876771268280445336693252758 74D+13	0.3D+12
k	D'_k	$\Delta D'_k$
0	−0.32883061871232049899140059583 19D+00	0.2D−27
1	0.13230380377457662132941302513 37D+00	0.2D−23
2	0.66271437033732752885946736249 92D+01	0.9D−20
3	−0.14487827869486890061092550261 77D+02	0.2D−16
4	0.55545449916102694038978312195 77D+02	0.3D−13
5	−0.26662260250999918697721639047 01D+03	0.3D−10
6	0.15108538335009243577556284181 47D+04	0.2D−07
7	−0.98961174347557737707367437772 409D+04	0.8D−05
8	0.73172441528362662668982393160 07D+05	0.3D−02
9	−0.60865770957524913748026264522 74D+06	0.6D+00
10	0.56403384158516212584637158409 17D+07	0.1D+03
11	−0.59178746294385246239102043074 28D+08	0.1D+05
12	0.69974551723653446526548309356 23D+09	0.1D+07
13	−0.94004100942344561797360986984 93D+10	0.8D+08
14	0.12212033560755751492938647504 61D+12	0.3D+10
15	−0.11524345879975847840540535562 44D+13	0.5D+11

such as $\ln S/S^2$, $\ln S/S^{5/2}$, ..., for the rhombus, trapezoid, and hexagon shapes, while such terms are absent for the triangle and rectangle shape. In the previous work [33], we have found the logarithmic corrections in higher order terms in the critical free energy for the rhombus, trapezoid and hexagon shapes (Table 13).

Note that the formula of perimeter $p(N) = (2 + \sqrt{3})N$ for the rectangular shape is only valid for odder number layers (see Fig. 1e), so, in our numerical calculations, the size N is set to be an odd number. For even number layer, it is expected that the results should be fitted with a different formula of perimeter. We have not studied this case.

For triangle and rectangle shapes, we fit the data with k from 1 to 13. We find that there is no logarithmic correction in higher orders, i.e., $u_{lk} = 0$. For rhombus, trapezoid and hexagon

Table 13 The fitted u_∞, edge, corner free energy density in Eq. (29) for the five shapes

Shape	u_∞	Δu_∞
Triangle	0.20000000000000000000000000001178D+01	0.1D−26
Rectangle	0.19999999999999999999999999998691D+01	0.1D−26
Rhombus	0.19999999999999999999999985951181D+01	0.2D−23
Trapezoid	0.19999999999999999999999999623657D+01	0.7D−24
Hexagon	0.19999999999999999999999998772999D+01	0.5D−23
Shape	u_{surf}	Δu_{surf}
Triangle	−0.55132889542179204951132741724 16D+00	0.1D−23
Rectangle	−0.55132889542179204951132393384 27D+00	0.2D−23
Rhombus	−0.55132889542179204945683672637 06D+00	0.7D−20
Trapezoid	−0.55132889542179204950964022726 82D+00	0.3D−20
Hexagon	−0.55132889542179204950215958684 56D+00	0.3D−19
Shape	u_{corn}	Δu_{corn}
Triangle	−0.16539866862653761485366461066 93D+01	0.5D−20
Rectangle	0.14772813229221208442252800295 59D+00	0.1D−19
Rhombus	−0.73510519389572183335350124115 74D+00	0.9D−16
Trapezoid	−0.73510519389572270014189184154 73D+00	0.7D−16
Hexagon	0.11026577908435843379274610991 24D+01	0.6D−15

shape, we fit the data with k from 1 to 9. We find that there are logarithmic corrections in higher orders. The higher order logarithmic corrections begins from $k = 4$ as listed in Table 14.

The bulk value U_∞ is known to be 2 [7]. Our fit of U_∞ is $2.0 + (3 \pm 9) \times 10^{-23}$ for the hexagonal shape, which is the worst among five cases. The best one is 2.0 ± 10^{-25} for the triangle shape. From this one can see the accuracy of the BP algorithm reaches 10^{-25} at least.

The leading correction is due to the edges (or surfaces), which is unknown to our knowledge. We denote the surface internal energy per unit length of the edge along one bond direction by $u^{\parallel}_{\text{surf}}$, and that perpendicular to that direction by $u^{\perp}_{\text{surf}}$. For the triangular, rhomboid, trapezoid, and hexagonal shapes (see Table 13) , we have $u_{\text{surf}} = u^{\parallel}_{\text{surf}}$. For the rectangular shape we have $u_{\text{surf}} = (2u^{\parallel}_{\text{surf}} + \sqrt{3}u^{\perp}_{\text{surf}})/(2 + \sqrt{3})$, and

$$\begin{aligned} u^{\parallel}_{\text{surf}} &= -0.55132889542179204951132 5(9), \\ u^{\perp}_{\text{surf}} &= -0.55132889542179204951131(1). \end{aligned} \tag{30}$$

This is an interesting result because it means that the surface internal energy per unit length is symmetric for an edge along or perpendicular to an arbitrary bond direction. We conjecture that the exact value of the surface internal energy is given by

$$u^{\parallel}_{\text{ex,surf}} = u^{\perp}_{\text{ex,surf}} = -\frac{\sqrt{3}}{\pi} = -0.55132889542179204951132 6\ldots \tag{31}$$

Following the convention for the critical free energy, we write the coefficient of $(\ln N)/S$ as u_{corn}. We denote the corner correction by $u^{(\gamma)}_{\text{corn}}$, where γ is the angle of the corner. Under the assumption that u_{corn} is the sum of the corner's contributions, we have

Table 14 The fitted parameters u_k in Eq. (29) and the refitted parameters u'_k in Eq. (34) for triangular shape

k	u_k	Δu_k
1	0.19206842404944072472443467895 82D+00	0.5D−22
2	−0.14880040323634737558619395569 85D+01	0.3D−19
3	−0.69061945461992495687004024503 56D+00	0.1D−17
4	−0.27249445261057300161929235270 22D−01	0.1D−15
5	0.16693575210889901311666913361 50D−01	0.1D−13
6	−0.95490230795676391395051718773 42D−02	0.8D−12
7	0.10239147218545619200021898063 31D−01	0.5D−10
8	−0.90927756400520913611347711336 74D−02	0.2D−08
9	0.24484887733199090173135916985 14D−02	0.7D−07
10	0.62095510295532859195376622585 66D−02	0.2D−05
11	−0.16432839189520585157187042053 44D−01	0.3D−04
12	0.28166239293127980998912969495 08D−01	0.3D−03
13	−0.28426355782195458860075050681 79D−01	0.2D−02
14	0.15774278409170497910682123182 37D−01	0.6D−02
k	u'_k	$\Delta u'_k$
1	0.19206842404944072472440261685 72D+00	0.2D−25
2	−0.14880040323634737558768063746 28D+01	0.3D−22
3	−0.69061945461992495632761775899 61D+00	0.2D−19
4	−0.27249445261057349921258944708 22D−01	0.5D−17
5	0.16693575210894693514154038692 32D−01	0.1D−14
6	−0.95490230799545771163913672684 04D−02	0.1D−12
7	0.10239147242824539189141917794 58D−01	0.9D−11
8	−0.90927767856276678468840832059 61D−02	0.5D−09
9	0.24485286189632382993885803405 58D−02	0.2D−07
10	0.62085503753875571828478553314 10D−02	0.6D−06
11	−0.16415254951041748105070399588 24D−01	0.1D−04
12	0.27961562731986680260437972998 00D−01	0.1D−03
13	−0.27010821596535895465038668873 13D−01	0.1D−02
14	0.11375328813491704960493043481 85D−01	0.3D−02

$$u_{\text{corn}} = \begin{cases} 3u_{\text{corn}}^{(\pi/3)} & \text{for triangle} \\ 2\left(u_{\text{corn}}^{(\pi/3)} + u_{\text{corn}}^{(2\pi/3)}\right) & \text{for rhombus and trapezoid} \\ 6u_{\text{corn}}^{(2\pi/3)} & \text{for hexagon} \\ 4u_{\text{corn}}^{(\pi/2)} & \text{for rectangle} \end{cases} \tag{32}$$

From the Table 13, we obtain the corner term for the three angles

$$\begin{aligned} u_{\text{corn}}^{(\pi/3)} &= -0.551328895421792049 51(1) \approx -\frac{\sqrt{3}}{\pi}, \\ u_{\text{corn}}^{(\pi/2)} &= 0.036932033073053021125(2) \approx \frac{1}{4\pi}(2\sqrt{3}-3), \\ u_{\text{corn}}^{(2\pi/3)} &= 0.1837762984739298(3) \approx \frac{1}{\sqrt{3}\pi}. \end{aligned} \tag{33}$$

Table 15 The fitted parameters u_k in Eq. (29) and the refitted parameters u'_k in Eq. (34) for rectangular shape

k	u_k	Δu_k
1	−0.11246230548818235164319766585 86D+01	0.6D−22
2	−0.12360999230771468948336585250 71D+01	0.6D−19
3	0.35200875730217130622896739092 61D+00	0.3D−17
4	−0.44819635101329142617408025258 91D−01	0.5D−15
5	0.14110818179121030903957121701 56D+00	0.6D−13
6	0.55256276100527142486819611882 74D−02	0.6D−11
7	0.10191755571483632997900586341 65D+00	0.5D−09
8	−0.28253575905213674115046228062 88D+00	0.3D−07
9	0.40414149305922489318520889441 27D+00	0.2D−05
10	−0.79604036273289333124644250777 72D+00	0.5D−04
11	0.18154325065442151562506850771 73D−01	0.1D−02
12	0.16682548551166691022193869340 27D+01	0.2D−01
13	−0.10743780868712973686907695421 44D+02	0.2D+00
14	0.12069280656641306500005665201 12D+02	0.8D+00
k	u'_k	$\Delta u'_k$
1	−0.11246230548818235164318939950 91D+01	0.1D−25
2	−0.12360999230771468947563915206 72D+01	0.3D−22
3	0.35200875730217130159053828196 87D+00	0.2D−19
4	−0.44819635101328503384689277854 75D−01	0.1D−16
5	0.14110818179112640228514791630 34D+00	0.3D−14
6	0.55256276188888082754745905487 04D−02	0.5D−12
7	0.10191755500095253084506477866 64D+00	0.5D−10
8	−0.28253571559556852625479439344 37D+00	0.4D−08
9	0.40413952779246457379970498930 51D+00	0.2D−06
10	−0.79597558721986887248575428804 41D+00	0.1D−04
11	0.16646504286370796104014209042 08D−01	0.3D−03
12	0.16917002584592509390846622651 63D+01	0.5D−02
13	−0.10962009735924564679275310948 94D+02	0.5D−01
14	0.12987963838927053241764943493 28D+02	0.2D+00

From this result, we conjecture that the exact result of $u_{\text{corn}}^{(\pi/3)}$ is $-\sqrt{3}/\pi$; $u_{\text{corn}}^{(\pi/2)}$ is $(2\sqrt{3}-3)/(4\pi)$;[1] $u_{\text{corn}}^{(2\pi/3)}$ is $1/(\sqrt{3}\pi)$

We redo the fitting for the data of critical internal energy with the formula given by

$$u = u_{\infty}^{\text{ex}} + u_{\text{surf}}^{\text{ex}} \frac{p(N)\ln N}{S} + \frac{u'_1}{S^{1/2}} + \frac{u_{\text{corn}}^{\text{ex}} \ln N + u'_2}{S} + \frac{u'_3}{S^{3/2}} + \sum_{k=3}^{\infty} \frac{u'_k + u'_{lk} \ln N}{S^{k/2}}, \quad (34)$$

where $u_{\infty}^{\text{ex}} = 2.0$, $u_{\text{surf}}^{\text{ex}} = -\sqrt{3}/\pi$ for all shapes and $u_{\text{corn}}^{\text{ex}}$ for each shape are given by Eqs. (32) and (33)

[1] The referee 2 told us that the conjectured values of $u_{\text{corn}}^{(\pi/2)}$, $c_{\text{surf}}^{(\perp)}$, $c_{\text{corn}}^{(\pi/2)}$ can be obtained with PSLQ integer relation algorithm. He provided the three values.

Table 16 The fitted parameters u_k in Eq. (29) and the refitted parameters u'_k in Eq.(34) for rhombus shape

k	u_k	Δu_k
1	−0.72860716620008588998078949908 44D+00	0.3D−18
2	−0.10933604462883890712499430371 32D+01	0.6D−15
3	−0.21973975453644532195792005660 98D+00	0.1D−12
4	0.67693863743489358615270404988 32D−01	0.4D−09
5	−0.16510279694882710791590328125 86D−01	0.1D−06
6	0.45758469953726818718055656238 19D−02	0.1D−04
7	−0.11308901431070173190695389089 31D+00	0.3D−03
8	0.13991335450611834895225925208 07D+00	0.1D−02
9	−0.10117466226964712864021405384 26D+00	0.1D−02
k	u_{lk}	Δu_{lk}
4	0.33564946968102411717662398012 72D−01	0.7D−10
5	−0.22377278933139399221497622915 20D−01	0.2D−07
6	0.17974130199883417496329249825 18D−01	0.3D−05
7	0.10388510118192594480906721791 77D−01	0.9D−04
8	0.12229179754682791529520368848 61D−01	0.9D−03
9	0.58201365804129244955588180630 59D−01	0.1D−02
k	u'_k	$\Delta u'_k$
1	−0.72860716620008588789957144846 21D+00	0.2D−21
2	−0.10933604462883826205850790819 61D+01	0.1D−17
3	−0.21973975453809659829579119371 78D+00	0.4D−14
4	0.67693857152048123076724309136 87D−01	0.6D−10
5	−0.16512459758305432319404867307 57D−01	0.3D−07
6	0.43723608977084870783834796012 33D−02	0.5D−05
7	−0.11866541789781134756946115999 14D+00	0.2D−03
8	0.10789104142692838644119598008 51D+00	0.1D−02
9	−0.75225622934861722469338129529 84D−01	0.9D−03
k	u'_{lk}	$\Delta u'_{lk}$
4	0.33564947930681883907136510925 89D−01	0.7D−11
5	−0.22376872450196894617551390974 45D−01	0.6D−08
6	0.18022473699120314682675066365 88D−01	0.1D−05
7	0.12221174665029874490965805412 35D−01	0.5D−04
8	0.31866022591392225978682284426 71D−01	0.7D−03
9	0.94149817450386215876788099399 78D−01	0.2D−02

In our fits for the internal energy density, the maximal deviation defined in Eq. (23) is $\delta_{max} < 10^{-29}, 10^{-29}, 10^{-27}, 10^{-28}, 10^{-28}$ for triangular, rectangular, rhomboid, trapezoid and hexagonal shape, respectively (Tables 14, 15, 16, 17, 18). In the refittings with the conjectured bulk, edge and corner terms, we have $\delta_{max} < 10^{-29}, 10^{-29}, 10^{-25}, 10^{-28}, 10^{-27}$ for triangular, rectangular, rhomboid, trapezoid and hexagonal shape, respectively.

Table 17 The fitted parameters u_k in Eq. (29) and the refitted parameters u'_k in Eq. (34) for trapezoid shape

k	u_k	Δu_k
1	−0.11882560455072204237023938476 95D+01	0.1D−18
2	−0.79635935093895677795415559671 87D+00	0.5D−15
3	0.96748380705831252451360914010 72D−03	0.2D−12
4	−0.11783517325633099060672108522 75D−01	0.1D−08
5	−0.16891859388444409703522675910 86D−01	0.5D−06
6	0.99726646305852827265767844475 59D−01	0.9D−04
7	−0.28072599658257794406249373488 22D+00	0.6D−02
8	0.10001589144347194655196634801 71D+00	0.1D+00
9	−0.21455548147864971440606711172 89D+01	0.5D+00
10	0.15604521851620020563547965827 93D+01	0.5D+00
k	u_{lk}	Δu_{lk}
4	0.42082943878452984861725128403 73D−01	0.1D−09
5	−0.49229278324861068955162283564 39D−01	0.9D−07
6	0.59731489205607287499598012077 67D−01	0.2D−04
7	−0.40468118418669415014555989890 83D−01	0.2D−02
8	0.15593845480817823739673146322 09D+00	0.4D−01
9	0.11573436406445956039843094701 16D+01	0.4D+00
10	0.20919350117398489550325033403 77D+01	0.7D+00
k	u'_k	$\Delta u'_k$
1	−0.11882560455072204236370737015 86D+01	0.6D−23
2	−0.79635935093895654672126493633 50D+00	0.6D−19
3	0.96748380698910461665439860136 37D−03	0.4D−15
4	−0.11783517657338049169639630772 17D−01	0.9D−11
5	−0.16891998997048399314718142618 15D−01	0.1D−07
6	0.99708911464615033365466461172 96D−01	0.3D−05
7	−0.28145428076836695997293638053 41D+00	0.3D−03
8	0.92322283045758014216791954659 69D−01	0.8D−02
9	−0.21446663969403768686353297794 76D+01	0.5D−01
10	0.15785629998595428251093627807 62D+01	0.4D−01
k	u'_{lk}	$\Delta u'_{lk}$
4	0.42082943926877298045733476144 84D−01	0.1D−11
5	−0.49229252563815712012270348346 65D−01	0.2D−08
6	0.59735583447601412826368652971 17D−01	0.6D−06
7	−0.40244450004624454828685357465 97D−01	0.7D−04
8	0.15979758499013051553311765086 44D+00	0.3D−02
9	0.11711608181359372781131010287 90D+01	0.3D−01
10	0.20846768460371694213266464608 74D+01	0.7D−01

There is no logarithmic corrections in higher order terms for the triangular and rectangular shapes. In contrast there are such terms for the rhombus, trapezoid and hexagon shapes. With the help of much more accurate data, we confirm the finding in the previous work [33] that,

Table 18 The fitted parameters u_k in Eq. (29) and the refitted parameters u'_k in Eq. (34) for hexagonal shape

k	u_k	Δu_k
1	−0.19917657442568280013430325893 99D+01	0.1D−17
2	−0.14626467145620730856292460301 67D−01	0.5D−14
3	−0.12947982119135148468434007214 87D+00	0.2D−11
4	0.34795214452364080854848051950 35D+00	0.1D−07
5	−0.26508354359782352975896761282 69D+00	0.9D−05
6	0.27200941636948709455249618219 85D+00	0.2D−02
7	−0.26306839313369130995408375956 99D+01	0.1D+00
8	−0.97238309919043154246245756233 20D+01	0.4D+01
9	−0.67859667680408099942351775352 61D+02	0.3D+02
10	0.33312882449565614837418868509 01D+02	0.2D+02
k	u_{lk}	Δu_{lk}
4	0.96786299595706793446992901118 02D−01	0.2D−08
5	−0.55881493927455202768190684160 01D−01	0.2D−05
6	0.64542381522530790371620761894 48D−01	0.4D−03
7	0.55655365428146099459222607036 97D+00	0.4D−01
8	0.67159638010693515534895461863 94D+01	0.2D+01
9	0.51872530690719145700712949289 16D+02	0.2D+02
10	0.12954670710355679592071261590 14D+03	0.5D+02
k	u'_k	$\Delta u'_k$
1	−0.19917657442568280010395780013 94D+01	0.3D−21
2	−0.14626467145618994325673177929 66D−01	0.3D−17
3	−0.12947982119222325562633156356 11D+00	0.2D−13
4	0.34795213669685141963691374154 46D+00	0.7D−09
5	−0.26508985011417564266858307728 32D+00	0.1D−05
6	0.27038263715874768312437391187 30D+00	0.4D−03
7	−0.27813435459185512861133278282 86D+01	0.5D−01
8	−0.14386808898062552155244072303 22D+02	0.2D+01
9	−0.10186461409586379799775675977 68D+03	0.2D+02
10	0.56874479495966394422414345173 20D+02	0.1D+02
k	u'_{lk}	$\Delta u'_{lk}$
4	0.96786300695875150733543213149 13D−01	0.9D−10
5	−0.55880392860364906006586971492 10D−01	0.2D−06
6	0.64888477991645589922947225031 79D−01	0.8D−04
7	0.59695742885681899940175977244 05D+00	0.1D−01
8	0.84474801906366939947166005092 76D+01	0.7D+00
9	0.75388797756670589497508292860 92D+02	0.1D+02
10	0.19499960834803253744858180779 87D+03	0.3D+02

for in critical free energy density, there is no logarithmic correction terms of order higher than $1/S$ for the triangular and rectangular shape, and there are such terms for the rhombus, trapezoid and hexagonal shape.

Table 19 The fitted A_0^{tri}, edge, corner specific heat in Eq. (35) for the five shapes

Shape	A_0^{tri}	ΔA_0^{tri}
Triangle	0.49906937804646044983367240220 04D+00	0.1D−26
Rectangle	0.49906937804646044983367242248 40D+00	0.1D−25
Rhombus	0.49906937804646044983231455186 57D+00	0.2D−21
Trapezoid	0.49906937804646044983365774515 44D+00	0.6D−23
Hexagon	0.49906937804646044983147073058 93D+00	0.1D−20
Shape	c_{surf}	Δc_{surf}
Triangle	0.16635645934882014999445687369 18D+00	0.2D−23
Rectangle	0.13809699167768709410533060405 23D+00	0.2D−22
Rhombus	0.16635645934882014181754436776 63D+00	0.8D−18
Trapezoid	0.16635645934882014980570780479 65D+00	0.5D−19
Hexagon	0.16635645934882012884856763343 23D+00	0.9D−17
Shape	c_{corn}	Δc_{corn}
Triangle	0.74860406706969067474917091060 39D+00	0.3D−20
Rectangle	−0.15004084808173595335331855659 68D+00	0.6D−19
Rhombus	0.38816507181377174344840049369 22D+00	0.1D−13
Trapezoid	0.38816507181390954523624153801 32D+00	0.1D−14
Hexagon	−0.33271291869810100951018091720 20D+00	0.1D−12

4.2 Critical Specific Heat Density

The data of the critical specific heat are fitted using the following formula

$$c = A_0^{\text{tri}} \ln N + c_0 + c_{\text{surf}} \frac{p(N) \ln N}{S} + \frac{c_1}{S^{1/2}} + \frac{c_{\text{corn}} \ln N + c_2}{S} + \sum_{k=3} \frac{c_k + c_{lk} \ln N}{S^{k/2}}, \quad (35)$$

where $p(N)$ is the perimeter. Compared with the expansion for the triangular lattice with periodic boundary conditions [13], there are additional logarithmic surface term and corner term.

The leading term $A_0^{\text{ex,tri}} \ln N$ is known from the exact result [13], which reads

$$A_0^{\text{ex,tri}} = \frac{3\sqrt{3}}{4\pi} (\ln 3)^2 = 0.49906937804646044983367 24\ldots \quad (36)$$

Our fits, listed in Table 19, agree with the exact result at least in accuracy 10^{-21}. The other fitted parameters are listed in Tables 20, 21, 22, 23 24 as well.

The leading correction $p(N) \ln N/S$ is caused by the edges. We denote the surface specific heat per unit length of the edge along one bond direction by $c_{\text{surf}}^{\parallel}$, and that perpendicular to the direction by $c_{\text{surf}}^{\perp}$. For the triangle, rhombus, trapezoid, and hexagon shape, we have $c_{\text{surf}} = c_{\text{surf}}^{\parallel}$; for the rectangle, we set $c_{\text{surf}} = (2c_{\text{surf}}^{\parallel} + \sqrt{3}c_{\text{surf}}^{\perp})/(2 + \sqrt{3})$, and find

Table 20 The fitted parameters c_k in Eq. (35) and the refitted parameters c'_k in Eq. (39) for triangular shape

k	c_k	Δc_k
0	−0.80424240621924908720063838051 13D+00	0.1D−25
1	−0.26569260021722084193832418100 88D+00	0.5D−22
2	0.73444549839129740030114257475 33D+00	0.2D−19
3	0.32466164625104135939083827471 57D+00	0.5D−18
4	0.16417025024422310125089633499 23D−01	0.4D−16
5	−0.78170199670988790487625400258 59D−02	0.3D−14
6	0.48860600223705152149622763003 34D−02	0.2D−12
7	−0.63546336422165750799042653810 69D−02	0.1D−10
8	0.50280524897271433822382105644 59D−02	0.4D−09
9	−0.22010321002860559262954331796 25D−02	0.1D−07
10	−0.25915721640087735650868203801 62D−02	0.3D−06
11	0.89448444165533355347310482233 80D−02	0.4D−05
12	−0.16328914830738714727165035869 40D−01	0.5D−04
13	0.22200326014940333541986785374 46D−01	0.3D−03
14	−0.16639173380518660733841265874 79D−01	0.9D−03
k	c'_k	$\Delta c'_k$
0	−0.80424240621924908720063838500 86D+00	0.3D−29
1	−0.26569260021722084193834369244 92D+00	0.7D−26
2	0.73444549839129740029388391309 09D+00	0.5D−23
3	0.32466164625104135962590811531 35D+00	0.2D−20
4	0.16417025024422292361498395117 64D−01	0.6D−18
5	−0.78170199670975294836873216222 82D−02	0.9D−16
6	0.48860600222856294829653302569 59D−02	0.1D−13
7	−0.63546336380324667833666137000 84D−02	0.8D−12
8	0.50280523319289666629172797346 87D−02	0.4D−10
9	−0.22010276271897009713407047834 62D−02	0.2D−08
10	−0.25916654334411317404270016200 73D−02	0.4D−07
11	0.89462282237163431864157426304 71D−02	0.8D−06
12	−0.16342715362263931171400861491 65D−01	0.9D−05
13	0.22283153322219100813370350584 66D−01	0.7D−04
14	−0.16865040099665544547247530548 35D−01	0.2D−03

$$
\begin{aligned}
c^{\parallel}_{\mathrm{surf}} &= 0.166356459348820149932(8) \approx \frac{A_0^{\mathrm{tri}}}{3}, \\
c^{\perp}_{\mathrm{surf}} &= 0.105465769143518701148(8) \approx \frac{A_0^{\mathrm{tri}}}{6}(3-\sqrt{3}).
\end{aligned} \tag{37}
$$

Note that this term is absent in the torus case [8] and not mentioned in the long strip case [9], but exists in the cylinder case with Brascamp-Kunz boundary conditions [14,11]. In addition, we conjecture that the exact result $c^{\parallel}_{\mathrm{surf}} = A_0^{\mathrm{tri}}/3$ and $c^{\perp}_{\mathrm{surf}} = A_0^{\mathrm{tri}}(3-\sqrt{3})/6$

Following the convention for the critical free energy, we write the coefficient of $\ln N/S$ as c_{corn}. We denote the corner correction by $c^{(\gamma)}_{\mathrm{corn}}$ where γ is the angle of the corner. Again, under the assumption that the total correction is the sum of all corners, we have

Table 21 The fitted parameters c_k in Eq. (35) and the refitted parameters c'_k in Eq. (39) for rectangular shape

k	c_k	Δc_k
0	−0.57338897908577661148117760783 06D+00	0.1D−24
1	−0.85347852280811837960521027565 95D−01	0.7D−21
2	0.65901330974134867970400439714 12D+00	0.3D−18
3	−0.19577904498324251695476387885 40D−01	0.1D−16
4	0.68155131508196301239178593335 80D−01	0.2D−14
5	−0.25366834268040363904381565967 63D−01	0.2D−12
6	0.75227435334882449298013250379 15D−01	0.2D−10
7	−0.16516098289933652468633502479 20D+00	0.1D−08
8	0.20707345803027726419558475606 71D+00	0.7D−07
9	−0.28515591281472024501993574258 81D+00	0.3D−05
10	−0.11357535809220896909940584437 20D+00	0.9D−04
11	0.87668964038915175726396839694 93D+00	0.2D−02
12	−0.40090164408667873982157034467 98D+01	0.3D−01
13	0.69534120433078464791735650506 99D+01	0.3D+00
14	−0.15421232777812909344955876582 83D+02	0.1D+01
k	c'_k	$\Delta c'_k$
0	−0.57338897908577661148117740172 83D+00	0.3D−27
1	−0.85347852280811837959413587937 45D−01	0.9D−24
2	0.65901330974134868028140307459 56D+00	0.1D−20
3	−0.19577904498324279284918370103 00D−01	0.6D−18
4	0.68155131508199529605470145372 37D−01	0.2D−15
5	−0.25366834268426099935762949719 11D−01	0.5D−13
6	0.75227435373317351492241869498 08D−01	0.8D−11
7	−0.16516098590434677814654830288 95D+00	0.9D−09
8	0.20707363747154519522335216464 84D+00	0.7D−07
9	−0.28516394040024997592677607853 99D+00	0.4D−05
10	−0.11331222718426901658546974486 21D+00	0.1D−03
11	0.87057771815771195548449911575 21D+00	0.4D−02
12	−0.39139786576994374411680401921 53D+01	0.6D−01
13	0.60675524225359831282948072865 60D+01	0.7D+00
14	−0.11683458153172600959456724021 32D+02	0.3D+01

$$c_{\text{corn}} = \begin{cases} 3c_{\text{corn}}^{(\pi/3)} & \text{for triangle} \\ 2\left(c_{\text{corn}}^{(\pi/3)} + c_{\text{corn}}^{(2\pi/3)}\right) & \text{for rhombus and trapezoid} \\ 6c_{\text{corn}}^{(2\pi/3)} & \text{for hexagon} \\ 4c_{\text{corn}}^{(\pi/2)} & \text{for rectangle} \end{cases}$$

From Table 19, we obtain the corner contribution of the three angles,

$$c_{\text{corn}}^{(\pi/3)} = 0.24953468902323021 7(3) \approx \frac{A_0^{\text{tri}}}{2},$$

$$c_{\text{corn}}^{(\pi/2)} = -0.03751021202043398 85(8) \approx \frac{A_0^{\text{tri}}}{24}(3\sqrt{3} - 7),$$

Table 22 The fitted parameters c_k in Eq. (35) and the refitted parameters c'_k in Eq. (39) for rhomboid shape

k	c_k	Δc_k
0	−0.60510340124288164836084375787 84D+00	0.2D−20
1	−0.14685068061459639184241123009 50D+00	0.3D−16
2	0.63737428195034753196675074629 03D+00	0.8D−13
3	0.14090528562872009791095276735 74D+00	0.8D−10
4	−0.24715874071402838486384360616 29D−01	0.3D−07
5	0.56304425365274701500744141529 04D−02	0.3D−05
6	−0.45164280379349362756875474150 61D−01	0.2D−03
7	−0.44761454340638745135629146695 81D−02	0.3D−02
8	−0.18513046618684524037557828194 46D+00	0.1D−01
9	0.17447907507431035219540558302 87D+00	0.1D−01
k	c_{lk}	Δ_{lk}
3	0.26942697910082684337584155809 23D−01	0.1D−10
4	−0.14044913077832831150962572414 02D−01	0.5D−08
5	0.11517999975591836661361025560 40D−01	0.7D−06
6	0.93100497960991701966852299054 91D−03	0.4D−04
7	0.37917278220465901605263869632 30D−01	0.1D−02
8	0.14819538012272785500974876196 87D+00	0.8D−02
9	0.14574605053382723669668789010 48D+00	0.1D−01
k	c'_k	$\Delta c'_k$
0	−0.60510340124288164837628319908 00D+00	0.1D−23
1	−0.14685068061459668741952373650 91D+00	0.1D−19
2	0.63737428194924877391417426562 14D+00	0.7D−16
3	0.14090528437758784313938182173 76D+00	0.2D−11
4	−0.24716387235556299748222810404 36D−01	0.2D−08
5	0.55500588443221205179689506342 31D−02	0.5D−06
6	−0.49898596331973192668608857362 72D−01	0.5D−04
7	−0.97497680194908073993994145614 92D−01	0.1D−02
8	−0.58395577110523320842040106220 28D+00	0.7D−02
9	0.55479748530132005178657288707 84D+00	0.6D−02
k	c'_{lk}	$\Delta c'_{lk}$
3	0.26942698097884911753488490584 00D−01	0.2D−12
4	−0.14044822986812238501268200002 51D−01	0.3D−09
5	0.11534856523342134455588990418 634D−01	0.1D−06
6	0.21710192540886764685164906688 13D−02	0.1D−04
7	0.71627603857046186351464781543 07D−01	0.4D−03
8	0.43019506422399847094463165753 94D+00	0.4D−02
9	0.57159809773075942840645342645 52D+00	0.8D−02

Table 23 The fitted parameters c_k in Eq. (35) and the refitted parameters c'_k in Eq. (39) for trapezoid shape

k	c_k	Δc_k
0	−0.51995022205995142577360111767 33D+00	0.7D−22
1	−0.84949996495774247083563740908 07D−01	0.2D−17
2	0.58836871614846551783417698555 60D+00	0.8D−14
3	0.21074972032123785554990294051 52D−01	0.1D−10
4	0.18697724452244313627596573852 42D−02	0.6D−08
5	0.11685008396829732292710288329 53D−01	0.1D−05
6	−0.63085239614360759204071816716 26D−01	0.2D−03
7	−0.59859210886180534497683943656 47D−01	0.6D−02
8	−0.16815120815484041755668288983 94D+01	0.1D+00
9	−0.34698675443578783423139606563 15D+01	0.3D+00
10	0.39571484478327362703289687854 20D+01	0.4D+00
k	c_{lk}	Δ_{lk}
3	0.29959640436168864756670133029 15D−01	0.2D−11
4	−0.23617751572710367417470757463 73D−01	0.1D−08
5	0.27340962255982256065166139049 20D−01	0.3D−06
6	−0.23112917486581806632793340685 51D−01	0.4D−04
7	0.94287922274399924682717423486 87D−01	0.2D−02
8	0.72377822416632877654585989553 49D+00	0.4D−01
9	0.39603376017543205532692017949 88D+01	0.3D+00
10	0.52740056295324150353778806532 16D+01	0.4D+00
k	c'_{lk}	$\Delta c'_k$
0	−0.51995022205995142577377139476 81D+00	0.3D−24
1	−0.84949996495774252407007848930 28D−01	0.5D−20
2	0.58836871614843215329615653015 14D+00	0.5D−16
3	0.21074971966491850935895042905 89D−01	0.2D−11
4	0.29959640445531973831910302382 82D−01	0.2D−12
5	0.18697241524811991968684681055 62D−02	0.4D−08
6	−0.23617743636303527009181479108 50D−01	0.6D−09
7	0.11670576348800186189159714400 53D−01	0.2D−05
8	0.27343725892438843782726044599 61D−01	0.4D−06
9	−0.64878906069476939300839145264 76D−01	0.4D−03
10	−0.22702728166276879881513796536 68D−01	0.8D−04
k	c'_{lk}	$\Delta c'_{lk}$
3	−0.14929558536332480762986031887 28D+00	0.3D−01
4	0.11994011125542812155774338860 48D+00	0.7D−02
5	−0.32460527388295792395899507096 21D+01	0.6D+00
6	0.13523567482228513136388971986 11D+01	0.2D+00
7	−0.96262329666038022441546359387 54D+01	0.3D+01
8	0.89835176852106160974232528486 20D+01	0.2D+01
9	0.10456310063297131079416316016 20D+02	0.3D+01
10	0.13249035464221919893549771822 27D+02	0.4D+01

Table 24 The fitted parameters c_k in Eq. (35) and the refitted parameters c'_k in Eq. (39) for hexagonal shape

k	c_k	Δc_k
0	−0.26733979383373518195955307726 27D+00	0.1D−19
1	−0.15907726045798496536266329983 71D+00	0.3D−15
2	0.40589777994416961777544157575 71D+00	0.1D−11
3	0.74686574584782825485459014665 41D−01	0.1D−08
4	−0.39802413782138748256615148797 90D−01	0.6D−06
5	0.43097640757591608184116240696 80D−01	0.1D−03
6	−0.85915422372196900758604678991 88D+00	0.9D−02
7	−0.31079390654902509707081184673 04D+01	0.3D+00
8	−0.21140553936668172266508472608 26D+02	0.2D+01
9	0.11814937231501255397685006960 82D+02	0.1D+01
k	c_{lk}	Δ_{lk}
3	0.78792700476338857734903276328 49D−01	0.2D−09
4	−0.37348411057358091685676126470 78D−01	0.1D−06
5	0.36716002501470884487504490839 67D−01	0.3D−04
6	0.18104445974148591517149826986 17D+00	0.3D−02
7	0.22461004542800742174379298127 94D+01	0.1D+00
8	0.16469419686324327560700376955 21D+02	0.1D+01
9	0.39783405914867395865153909891 50D+02	0.3D+01
k	c'_k	$\Delta c'_k$
0	−0.26733979383373518198403562500 49D+00	0.4D−23
1	−0.15907726045798561530010198299 90D+00	0.5D−19
2	0.40589777994067979485237163583 97D+00	0.5D−15
3	0.74686568695174951041935319717 41D−01	0.2D−10
4	−0.39806068501245606460380817921 34D−01	0.3D−07
5	0.42214550258350982884650154552 14D−01	0.1D−04
6	−0.94109080411067190311769974941 65D+00	0.2D−02
7	−0.57230479346283991103612932336 89D+01	0.7D−01
8	−0.41154667724746566696393234996 27D+02	0.7D+00
9	0.24972026756190824516116166064 91D+02	0.4D+00
k	c'_{lk}	$\Delta c'_{lk}$
3	0.78792701380009104313117128411 69D−01	0.2D−11
4	−0.37347755119382509451492187244 13D−01	0.4D−08
5	0.36905292547040452430231675092 23D−01	0.2D−05
6	0.20295155545028185727321689809 60D+00	0.4D−03
7	0.32063125364820109328551152890 75D+01	0.2D−01
8	0.29977269334544296395618743760 79D+02	0.4D+00
9	0.78790005374342795091828981791 60D+02	0.1D+01

$$c_{\text{corn}}^{(2\pi/3)} = -0.05545215311627(5) \approx \frac{A_0^{\text{tri}}}{9}. \tag{38}$$

We conjecture that $c_{\text{corn}}^{(\pi/3)} = A_0^{\text{tri}}/2$, $c_{\text{corn}}^{(\pi/2)} = \frac{A_0^{\text{tri}}}{24}(3\sqrt{3}-7)$ and $c_{\text{corn}}^{(2\pi/3)} = A_0^{\text{tri}}/9$.

We redo the fitting with the conjectured exact leading logarithmic term, the surface term and the corner terms in the following way

$$c = A_0^{\text{ex,tri}} \ln N + c_0 + c_{\text{surf}}^{\text{ex}} \frac{p(N) \ln N}{S} + \frac{c_1}{S^{1/2}} + \frac{c_{\text{corn}}^{\text{ex}} \ln N + c_2}{S} + \sum_{k=3} \frac{c_k + c_{lk} \ln N}{S^{k/2}}, \tag{39}$$

The fitting results are shown in Tables 20, 21, 22, 23 24. We can see that the accuracy of the other fitted parameters increase, especially for the low order terms.

In our fittings for the internal energy density, the maximal deviation defined in Eq. (23) is $\delta_{max} < 10^{-30}, 10^{-29}, 10^{-27}, 10^{-29}, 10^{-27}$ for triangular, rectangular, rhomboid, trapezoid and hexagonal shape respectively. In the refittings with the conjectured bulk, edge and corner terms, we have $\delta_{max} < 10^{-30}, 10^{-28}, 10^{-25}, 10^{-27}, 10^{-26}$ for triangular, rectangular, rhomboid, trapezoid and hexagonal shape respectively.

For triangle and rectangle shape, we fit the data with k from 1 to 14. We find that there is no logarithmic correction in higher order terms, i.e. $c_{lk} = 0$. Therefore there is no c_{lk} in Tables 20 and 21. For rhombus, trapezoid and hexagon shape, we fit the data with k from 1 to 9. We find that there are logarithmic correction in higher order terms. The higher order logarithmic corrections begins from $k = 3$ as shown in Tables 22, 23 and 24.

5 BP Algorithm for Specific Heat

We consider the partition function of the Ising model on a 2D lattice

$$Z = \sum_{\{\sigma\}} e^{-\beta H}, \tag{40}$$

where the Hamiltonian is given by

$$\beta H = -\sum_{\langle ij \rangle} J_{ij} \sigma_i \sigma_j, \tag{41}$$

where $J_{ij} = \beta K_{ij}$ and $K_{ij} = K$ are the homogeneous couplings. The free energy density is defined as

$$f = \frac{F}{S} = \frac{\ln Z}{S}, \tag{42}$$

where F, S are the total free energy and number of spins or the area of the system respectively.

The internal energy density and specific heat density can be computed from

$$u = \frac{U}{S} = \frac{\partial f}{\partial \beta} = -\frac{1}{SZ} \sum_{\{\sigma\}} \left(H e^{-\beta H} \right), \tag{43}$$

and

$$c = \frac{C}{S} = \beta^2 \frac{\partial^2 f}{\partial \beta^2} = \frac{\beta^2}{S} \left(\sum_{\{\sigma\}} H^2 e^{-\beta H}/Z - U^2 \right), \tag{44}$$

where U, C are the total internal energy and heat capacity. Note here the definition of internal energy is different from the ordinary one in the sign.

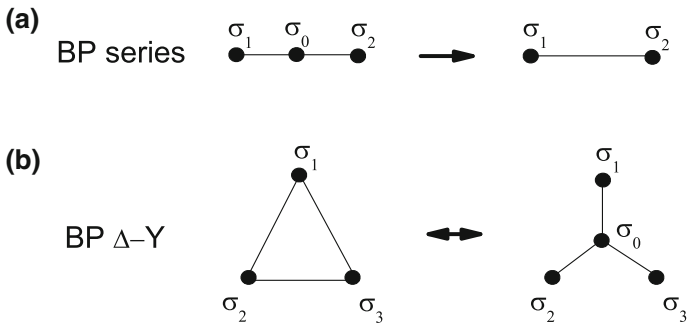

Fig. 2 **a**, **b** are building blocks of the BP algorithm: BP series and BP $\Delta - Y$ transformation, respectively

Along the the same route as the BP algorithm for the internal energy in [31], we develop the BP algorithm for the specific heat. Using these algorithm, we can avoid numerical differentiation used in previous works [32,33] and obtain much accurate results. For the convenience of the interested readers, we give the details of our algorithm here.

The scheme of the BP algorithm is given in [30,31]. Two main transformations: BP series reduction and BP $Y - \Delta$ transformation, as shown in Fig. 2, are the building blocks. To calculate the free energy the transformations preserve Z. To calculate the internal energy other transformations preserving $Z' \equiv \Sigma_{\{\sigma\}} H \mathrm{e}^{-\beta H}$ are needed. In order to use the BP algorithm to calculate the specific heat directly, we further need corresponding transformations which preserve $Z'' \equiv \sum_{\{\sigma\}} H^2 \mathrm{e}^{-\beta H}$. The procedure is equivalent to do transformations preserving the following quantity

$$\sum_{\{\sigma\}} \left[\left(\sum_{<ij>} J'_{ij} \sigma_i \sigma_j + U \right)^2 + \sum_{<ij>} J''_{ij} \sigma_i \sigma_j + C \right] e^{F + \sum\limits_{<ij>} J_{ij} \sigma_i \sigma_j}, \tag{45}$$

in which new couplings J' and J'' are introduced with initial values $J'_{ij} = K_{ij}$, $J''_{ij} = 0$. F, U and C is set to zero initially. All couplings and F, U, C change values in each step. As the transformations are completed, i.e., all bonds are eliminated by the BP algorithm, the final results of F, U and C are obtained as the total free energy, internal energy and heat capacity, respectively.

At first, let us discuss the BP "series" reduction for the specific heat. It corresponds to integrating out a spin with two neighbors, generating effective couplings J_{12}, J'_{12}, J''_{12} such that

$$\begin{aligned} \sum_{\sigma_0} & e^{J_{10}\sigma_0\sigma_1 + J_{20}\sigma_0\sigma_2 + H_{\mathrm{ex}}} \left[\left(J'_{10}\sigma_0\sigma_1 + J'_{20}\sigma_0\sigma_2 + H'_{\mathrm{ex}} \right)^2 + J''_{10}\sigma_0\sigma_1 + J''_{20}\sigma_0\sigma_2 + H''_{\mathrm{ex}} \right] \\ & = e^{J_{12}\sigma_1\sigma_2 + H_{\mathrm{ex}} + \delta F} \left[\left(J'_{12}\sigma_1\sigma_2 + H'_{\mathrm{ex}} + \delta U \right)^2 + J''_{12}\sigma_1\sigma_2 + H''_{\mathrm{ex}} + \delta C \right], \end{aligned} \tag{46}$$

where the quadratic terms not involving σ_0 are collected in $H_{\mathrm{ex}}(\sigma_1, \sigma_2, \ldots, F)$, $H'_{\mathrm{ex}}(\sigma_1, \sigma_2, \ldots, U)$ and $H''_{\mathrm{ex}}(\sigma_1, \sigma_2, \ldots, C)$, respectively, according to the couplings. In each step, we have $F \to F + \delta F$, $U \to U + \delta U$ and $C \to C + \delta C$. Since H'_{ex} and H''_{ex} contain the variables $\sigma_1, \sigma_2, \cdots, U$ and C, the prefactors of them in both sides of the above equation must be equal. Equating the prefactors of H'^2_{ex}, or H''_{ex}, in both sides of the above equation yields

$$\sum_{\sigma_0} e^{J_{10}\sigma_1\sigma_0+J_{20}\sigma_2\sigma_0} = e^{\delta F+J_{12}\sigma_1\sigma_2}. \tag{47}$$

This is the BP series transformation for the partition function [30,31], which requires

$$e^{\delta F\pm J_{12}} = 2\cosh(J_{10}\pm J_{20}) \equiv a_{\pm}. \tag{48}$$

The solution is given by

$$\delta f = \sqrt{a_+a_-},\ j_{12} = \sqrt{a_+/a_-}, \tag{49}$$

with $\delta f = e^{\delta F}$ and $j_{ij} = e^{-J_{ij}}$.

Equating the prefactors of $H'_{\rm ex}$ in the two sides of Eq. (46) yields

$$\begin{aligned}\sum_{\sigma_0} &\left[J'_{10}\sigma_1\sigma_0 + J'_{20}\sigma_2\sigma_0\right]e^{J_{10}\sigma_1\sigma_0+J_{20}\sigma_2\sigma_0}\\ &= \left[J'_{12}\sigma_1\sigma_2 + \delta U\right]e^{\delta F+J_{12}\sigma_1\sigma_2},\end{aligned} \tag{50}$$

which leads to

$$e^{\delta F\pm J_{12}}(\delta U \pm J'_{12}) = 2(J'_{10}\pm J'_{20})\sinh(J_{10}\pm J_{20}). \tag{51}$$

Substituting Eq. (48) into above equation, we obtain

$$\delta U \pm J'_{12} = (J'_{10}\pm J'_{20})\tanh(J_{10}\pm J_{20}) \equiv a'_{\pm}, \tag{52}$$

with solution given by

$$\delta U = \frac{1}{2}(a'_+ + a'_-),\ J'_{12} = \frac{1}{2}(a'_+ - a'_-). \tag{53}$$

In fact these transformations are the BP series reduction for the internal energy. Although the $Y-\Delta$ transformations for the internal energy has been discussed in [31], this transformation was not given.

The rest terms in both sides of Eq. (46) also should be equal, which means

$$\begin{aligned}\sum_{\sigma_0} &e^{J_{10}\sigma_1\sigma_0+J_{20}\sigma_2\sigma_0}\left[(J'_{10}\sigma_1\sigma_0 + J'_{20}\sigma_2\sigma_0)^2 + J''_{10}\sigma_1\sigma_0 + J''_{20}\sigma_2\sigma_0\right]\\ &= e^{\delta F+J_{12}\sigma_1\sigma_2}\left[(J'_{12}\sigma_1\sigma_2 + \delta U)^2 + J''_{12}\sigma_1\sigma_2 + \delta C\right].\end{aligned} \tag{54}$$

This leads to

$$\begin{aligned}2\ \ &(J'_{10}\pm J'_{20})^2\cosh(J_1\pm J_2) + 2(J''_{10}\pm J''_{20})\sinh(J_1\pm J_2)\\ &= e^{\delta F\pm J_{12}}\left[(\delta U\pm J'_{12})^2 \pm J''_{12} + \delta C\right].\end{aligned} \tag{55}$$

Substituting Eqs. (48) and (51) into the above equation, we have

$$\delta C = (a''_+ + a''_-)/2, \qquad J''_{12} = (a''_+ - a''_-)/2, \tag{56}$$

where

$$a''_{\pm} = (J'_{10}\pm J'_{20})^2 + (J''_{10}\pm J''_{20})\tanh(J_{10}\pm J_{20}) - (a'_{\pm})^2. \tag{57}$$

Eqs. (49), (53) and (56) are the transformations of the BP series reduction for the specific heat.

The BP $Y-\Delta$ transformation corresponds to integrating the center spin, generating effective couplings J_{12}, J_{23}, J_{31}, J'_{12}, J'_{23}, J'_{31}, and J''_{12}, J''_{23}, J''_{31} such that

$$
\begin{aligned}
&e^{J_{12}\sigma_1\sigma_2+J_{23}\sigma_2\sigma_3+J_{31}\sigma_3\sigma_1+\delta F}\big[(J'_{12}\sigma_1\sigma_2+J'_{23}\sigma_2\sigma_3+J'_{31}\sigma_3\sigma_1+H'_{\rm ex}+\delta U)^2\\
&\quad+J''_{12}\sigma_1\sigma_2+J''_{23}\sigma_2\sigma_3+J''_{31}\sigma_3\sigma_1+H''_{\rm ex}+\delta C\big]\\
&=\sum_{\sigma_0}e^{J_{10}\sigma_0\sigma_1+J_{20}\sigma_0\sigma_2+J_{30}\sigma_0\sigma_3}\big[(J'_{10}\sigma_0\sigma_1+J'_{20}\sigma_0\sigma_2+J'_{30}\sigma_0\sigma_3+H'_{\rm ex})^2\\
&\quad+J''_{10}\sigma_0\sigma_1+J''_{20}\sigma_0\sigma_2+J''_{30}\sigma_0\sigma_3+H''_{\rm ex}\big],\quad\forall\sigma_1,\sigma_2,\sigma_3.
\end{aligned}
\tag{58}
$$

where $H'_{\rm ex}(\sigma_1,\sigma_2,\ldots,U)$ and $H''_{\rm ex}(\sigma_1,\sigma_2,\ldots,C)$ collect the quadratic terms not involving σ_0 with couplings J' and J'', respectively. Similarly the prefactors of $H'_{\rm ex}$ and $H''_{\rm ex}$ in both sides of above equation should be equal. Equating the prefactor of $H'^2_{\rm ex}$ and $H''_{\rm ex}$ in both sides of the above equation, we obtain the solution for δF, J_{12}, J_{23}, J_{31}

$$
\begin{aligned}
\delta f &= (b_0b_1b_2b_3)^{1/4},\\
j_{12} &= \big[b_1b_2/(b_0b_3)\big]^{-1/4}\quad(cycl.),
\end{aligned}
\tag{59}
$$

where $\delta f=e^{\delta F}$, $j_{ij}=e^{-J_{ij}}$, and

$$
\begin{aligned}
b_0 &= 2\cosh(J_{10}+J_{20}+J_{30}),\\
b_1 &= 2\cosh(J_{20}+J_{30}-J_{10})\quad(cycl.),
\end{aligned}
\tag{60}
$$

where "cylc." means that j_{31}, j_{12}, b_2, b_3 are related to those above by cyclic permutations of the indices 1, 2, 3.

The transformation for δU, j'_{12}, j'_{23}, j'_{31} is given by

$$
\begin{aligned}
\delta U &= \frac{1}{4}(b'_0+b'_1+b'_2+b'_3),\\
J'_{12} &= \frac{1}{4}(b'_0-b'_1-b'_2+b'_3)\quad(cycl.),
\end{aligned}
\tag{61}
$$

where

$$
\begin{aligned}
b'_0 &= (J'_{10}+J'_{20}+J'_{30})\tanh(J_{10}+J_{20}+J_{30}),\\
b'_1 &= (J'_{20}+J'_{30}-J'_{10})\tanh(J_{20}+J_{30}-J_{10}).\\
&\quad(cycl.)
\end{aligned}
\tag{62}
$$

The transformation for δC, j''_{12}, j''_{23}, j''_{31} is

$$
\begin{aligned}
\delta C &= \frac{1}{4}(b''_0+b''_1+b''_2+b''_3),\\
J''_{12} &= \frac{1}{4}(b''_0-b''_1-b''_2+b''_3)\quad(cycl.),
\end{aligned}
\tag{63}
$$

where

$$
\begin{aligned}
b''_0 &= (J'_{10}+J'_{20}+J'_{30})^2[1-\tanh^2(J_{10}+J_{20}+J_{30})]\\
&\quad+(J''_{10}+J''_{20}+J''_{30})\tanh(J_{10}+J_{20}+J_{30}),\\
b''_1 &= (J'_{20}+J'_{30}-J'_{10})^2[1-\tanh^2(J_{20}+J_{30}-J_{10})]\\
&\quad+(J''_{20}+J''_{30}-J''_{10})\tanh(J_{20}+J_{30}-J_{10}).\quad(cycl.)
\end{aligned}
\tag{64}
$$

The BP Δ-Y transformation corresponds to inserting a new spin, generating effective couplings J_{10}, J_{20}, J_{30}, J'_{10}, J'_{20}, J'_{30}, and J''_{10}, J''_{20}, J''_{30}, such that

$$\sum_{\sigma_0} e^{J_{10}\sigma_0\sigma_1+J_{20}\sigma_0\sigma_2+J_{30}\sigma_0\sigma_3+\delta F}\big[(J'_{10}\sigma_0\sigma_1+J'_{20}\sigma_0\sigma_2+J'_{30}\sigma_0\sigma_3+H'_{\rm ex}+\delta U)^2$$
$$+J''_{10}\sigma_0\sigma_1+J''_{20}\sigma_0\sigma_2+J''_{30}\sigma_0\sigma_3+H''_{\rm ex}+\delta C\big]$$
$$= e^{J_{12}\sigma_1\sigma_2+J_{23}\sigma_2\sigma_3+J_{31}\sigma_3\sigma_1}\big[(J'_{12}\sigma_1\sigma_2+J'_{23}\sigma_2\sigma_3+J'_{31}\sigma_3\sigma_1+H'_{\rm ex})^2$$
$$+J''_{12}\sigma_1\sigma_2+J''_{23}\sigma_2\sigma_3+J''_{31}\sigma_3\sigma_1+H''_{\rm ex}\big],\quad \forall\sigma_1,\sigma_2,\sigma_3. \tag{65}$$

Similar to the procedure in the $Y-\Delta$ transformation, we obtain the solution for $\delta F, J_{10},\ldots,\delta U,\ldots$ Using the variables $\delta f = e^{\delta F}$, $j_i = e^{-J_{i0}}$, $j_{ij} = e^{-J_{ij}}$, the solution for $\delta F, J_{10}, J_{20}, J_{30}$ is given by

$$j_i = \sqrt{(1-t_i)/(1+t_i)},\quad i=1,2,3$$
$$\delta f = z_0/\big[j_1j_2j_3+1/(j_1j_2j_3)\big], \tag{66}$$

where

$$t_1 = \sqrt{c_2c_3/(c_0c_1)}\ \ (cycl.), \tag{67}$$

with

$$c_0 = z_0+z_1+z_2+z_3,$$
$$c_1 = z_0+z_1-z_2-z_3\ \ (cycl.), \tag{68}$$

and

$$z_0 = 1/(j_{12}j_{23}j_{31}),$$
$$z_1 = j_{12}j_{31}/j_{23}\quad (cycl.). \tag{69}$$

The solution for $\delta U, J'_{10}, J'_{20}, J'_{30}$ is given by

$$\delta U = (z'_1+z'_2+z'_3-z'_0)/(c'_1+c'_2+c'_3-c'_0),$$
$$J'_1 = \frac{1}{2}\big[(z'_0-z'_1)-(c'_0-c'_1)\delta U\big]\quad (cycl.), \tag{70}$$

with

$$c'_0 = \coth(J_{10}+J_{20}+J_{30}),$$
$$c'_1 = \coth(J_{20}+J_{30}-J_{10})\quad (cycl.), \tag{71}$$

and

$$z'_0 = c'_0(J'_{12}+J'_{23}+J'_{31}),$$
$$z'_1 = c'_1(J'_{23}-J'_{12}-J'_{31})\quad (cycl.). \tag{72}$$

.

The solution for $\delta C, J''_{10}, J''_{20}, J''_{30}$ is given by

$$\delta C = (z''_1+z''_2+z''_3-z''_0)/(c'_1+c'_2+c'_3+c'_0),$$
$$J''_1 = \frac{1}{2}\big[(z''_0-z''_1)-(c'_0-c'_1)\delta C\big]\quad (cycl.), \tag{73}$$

where

$$z''_0 = c'_0\big[J''_{12}+J''_{23}+J''_{31}+(c'^{-2}_0-1)(J'_{12}+J'_{23}+J'_{31})^2\big],$$
$$z''_1 = c'_0\big[J''_{23}-J''_{12}-J''_{31}+(c'^{-2}_1-1)(J'_{23}-J'_{12}-J'_{31})^2\big]\quad (cycl.). \tag{74}$$

6 Conclusion and Discussions

We have developed the BP algorithm for the specific heat and made the BP algorithm for the internal energy completed. With these algorithm, we have studied the surface and corner quantities via a numerically exact approach on 2D lattices with free boundaries, which permits us to extract very precisely many terms in their asymptotic expansions, and sometimes even allows conjectures of their exact values. This work is a continuation of earlier works [32, 33] by the three of the present authors, but here addressing specifically the internal energy and the specific heat. There are two remarkable progresses comparing with previous work [32,33]:

(I) Some exact edge and corner terms are conjectured from the accurate numerical fits. For the rectangular shape on the square lattice, the exact edge term and corner term of internal energy and specific heat $u_{\rm surf}$, $u_{\rm corner}$, $c_{\rm surf}$, $c_{\rm corn}$ are conjectured. From the results for various shapes on the triangular lattice, we conjectured the exact edge and corner terms $u^{\parallel}_{\rm surf}$, $u^{\perp}_{\rm surf}$,$u^{(\pi/3)}_{\rm corn}$, $u^{(2\pi/3)}_{\rm corn}$,$u^{(\pi/2)}_{\rm corn}$, $c^{\parallel}_{\rm surf}$,$c^{(\pi/3)}_{\rm corn}$, $c^{(2\pi/3)}_{\rm corn}$, $c^{(\pi/2)}_{\rm corn}$. These conjectured exact results imply that there should exist closed form analytical solutions for these cases with free boundaries.

(II) The accurate forms of finite-size scaling for the internal energy and specific heat are determined. For the rectangular shape on the square and triangular lattice, there is no logarithmic correction terms of order higher than $1/S$. For the triangle shape on the triangular lattice, there is also no logarithmic correction terms higher that $1/S$. For the rhombus, trapezoid and hexagonal shape on the triangular lattice, there exist logarithmic correction terms of order higher than $1/S$ for the internal energy, and logarithmic correction terms of all orders for the specific heat. This property seems harmonic. The origin of these higher order logarithmic corrections are an interesting topic for the RG and CFT.

For the free energy, there is an universal corner term, an additional logarithmic correction. This is predicted by Cardy and Peschel [4] with in CFT. Privman proposed a mechanism to incorporate this universal logarithmic correction into the finite size scaling theory [2]. When the dimensionality passes through an integer value, $D = 2$ here, the singular $\sim L^{-D}$ and nonsingular $\sim L^{-2}$ terms in the free energy may have divergent amplitudes yielding additional logarithmic factors. In the previous work on Ising model on the square lattice and triangle lattice [32,33], our numerical results agree with this conclusion very well. In this work, our numerical results show the logarithmic corrections in the edge and corner terms clearly. The amplitudes of these terms should be related to the singular part of the free energy in certain way. How to incorporate these results into the finite size scaling theory is an interesting problem.

With Vernier and Jacobsen's analytical solution [29], one can study the internal energy and specific heat. However this calculation has not been carried out. It should be also interesting to compare the results obtained by their solution and our numerical results with the BP algorithm.

Acknowledgments This work is supported by the National Science Foundation of China (NSFC) under Grant No. 11175018. N.I. is also supported by a Marie Curie IIF (Project no. 300206-RAVEN) and IRSES (Projects no. 295302-SPIDER and 612707-DIONICOS) within 7th European Community Framework Programme and by the grant of the Science Committee of the Ministry of Science and Education of the Republic of Armenia under contract 13-1C080.

Appendix 1: Raw Data

In this appendix, we present some selected raw data of internal energy density on square lattice in Table 25. With these data, the future readers can check out fittings. Similarly, we present some selected raw data for specific heat calculated by BP algorithm in Table 26. In Table 27, we present some selected raw data of the internal energy density on triangle lattice for the five shapes. The Table 28 are some selected raw data of the specific heat on triangle lattice for the five shapes.

Table 25 Some selected raw data of the free energy density for $\rho = 1, 2, 4, 8, 16$

N	u for $\rho = 1$
30	1.261307730324047741285264873988 24
100	1.353851567390970699721879008338 37
2000	1.409312038870669142063944552104 16
N	u for $\rho = 2$
30	1.289998322139341458468575941825 92
100	1.365923114226176421511409979992 83
2000	1.410381610140965420763830853805 38
N	u for $\rho = 4$
30	1.304386406910265519805009670578 26
100	1.371971428318587034380337971396 89
1800	1.410597251612727191707878122094 50
N	u for $\rho = 8$
30	1.311580525039093715190022015379 46
100	1.374995605403185014100211797151 19
1350	1.409934688374894397823215622017 37
N	u for $\rho = 16$
30	1.315177584103824821961862919572 66
100	1.376507693945551791023858806519 38
1000	1.408892023206895097266910625739 53

Table 26 Some selected raw data of the specific heat for $\rho = 1, 2, 4, 8, 16$

N	c for $\rho = 1$
30	1.210940415343340597183519448591 08
100	1.748425886894339283218361682247 56
2000	3.191792603941777116968880079180 91
N	c for $\rho = 2$
30	1.322019252698942159882373223843 50
100	1.868542159078508863171426007585 71
2000	3.319037146002963770588552867951 21

Table 26 continued

N	c for $\rho = 4$
30	1.37869625861952258162210268572306
100	1.76287519298747414147215824745287
1800	3.33188166351652573000626009574603
N	c for $\rho = 8$
30	1.40703816618119026517435860483502
100	1.96028632460944206617378735484173
1350	3.25780716447088811708536457549625
N	c for $\rho = 16$
30	1.42120911998844802511367464421776
100	1.97557801603751029104177337576223
1000	3.09129554053638858398204013715747

Table 27 Some selected raw data of the internal energy density for the five shapes

N	u for triangle shape
30	1.63060227492790868278537498347110
100	1.85006839416789286050568941801225
2000	1.98756324359872297777008621627787
N	u for rectangular shape
31	1.73113619694831814565745047520278
103	1.89596983217880922846757982641780
1999	1.99161219443700093675294969789963
N	u for rhomboid shape
32	1.73482374548212137939580538377306
100	1.89070731063735122519011092404766
2000	1.99125283186916577248235926650852
N	u for trapezoid shape
32	1.76744633273493715838195345546356
100	1.90525667879528503501701486530454
1950	1.99236125763655109113034986398112
N	u for hexagonal shape
32	1.84153989080574954800859874234452
100	1.93732278606802211080066734935926
1240	1.99273490078456202139690918612710

Table 28 Some selected raw data of the specific heat for the five shapes

N	c for triangle shape
30	0.997469189513604027255498456670444
100	1.536658083954461563196145768385 74
2000	2.992742123455047732742080850026 10
N	c for rectangular shape
31	1.195781760205582066529755686223 27
103	1.762131243488873657458295672953 66
1999	3.221656302212303309797470249946 38
N	c for rhomboid shape
32	1.193961885239757774107557640479 62
100	1.722614262886403740955095771563 82
2000	3.190730651922326229815105135847 66
N	c for trapezoid shape
32	1.269097636619006654856801839990 04
100	1.803384260652969192017393316835 23
1950	3.262911560635780708388269985844 17
N	c for hexagonal shape
32	1.496322583697603646872929324505 61
100	2.045474988923357873128201970275 20
1240	3.289303043677739278563011884796 42

Appendix 2: Some Data Beyond the Fitting Size Range

In Sect. 3.1, we fit the critical internal energy density on square lattice with the size range from $N \geq 30$. We can predict the data outside this range. This would provide one additional diagnostic on our choice of functional form.

In Table 29, we present the internal energy density obtained by the fitting formula Eq. (18) with size $N = 5, 10, 15, 20$. For comparison, we also calculate these data with BP algorithm. Since the sizes of lattice are very small, the errors due to the accumulation of round-off error are less than 10^{-31}. Because the fitting formula Eq. (18) is only expanded to 15th order, the truncation error should be proportional to N^{-16}. They are about 6.0×10^{-12}, 10^{-16}, 10^{-19} and 2.0×10^{-21} for $N = 5, 10, 15, 20$ respectively. These truncation errors are much larger than the errors in the BP algorithm. Therefore we can take the data obtained with BP algorithm as more accurate values to check the truncation errors of the data obtained by the fitting formula Eq. (18). Take the internal energy density as an example, see Table 29. The absolute values of difference between the data obtained with Eq. (18) and data obtained with BP algorithm are about 4×10^{-10}, 3×10^{-13}, 3×10^{-17}, and 5×10^{-20} for $N = 5, 10, 15,$ and 20, for $\rho = 1$. They agree with the truncation errors estimated above approximately. It is so for other cases.

Table 29 The internal energy density of the systems with size beyond our fitting data. The left column are obtained with the fitting formula (18) and the right column are obtained with BP algorithm

	Data obtained with Eq. (18)	Data obtained with BP algorithm
N	u for $\rho = 1$	
5	0.88027559219944951337544040216836 9	0.88027559501494212257428716678426 1
10	1.07801112830089766249929303315032 3	1.07801112830062958702516944632988 7
15	1.16094890832628158774008024494375 8	1.16094890832628152380987852580355 2
20	1.20818582167072851402823002716610 6	1.20818582167072851397602671271849 9
N	u for $\rho = 2$	
5	0.96796208871733661496442299136572 6	0.96796208785778530403123087217945 7
10	1.13638127701183958314482754668873 5	1.13638127701176480235239794874795 2
15	1.20628712569666826805508763560319 9	1.20628712569666825014013629657039 8
20	1.24582855183024616298100379361325 0	1.24582855183024616296609765228158 5
N	u for $\rho = 4$	
5	1.01214338590956090621464974227617 0	1.01214338391157441576107244389866 9
10	1.16570772945159868920785145280554 4	1.16570772945155528072835745579768 2
15	1.22904565433706598794922224922816 4	1.22904565433706597751343609381919 0
20	1.26471543766273826112792377902446 6	1.26471543766273826111903809021370 5
N	u for $\rho = 8$	
5	1.03423533071121061304686135603450 9	1.03423532832650532078415276256901 2
10	1.18037129629809539409946968895707 8	1.18037129629806881232422436821844 7
15	1.24042510298243688539627739778332 5	1.24042510298243687909671302699027 0
20	1.27415900565258094343132629719732 5	1.27415900565258094342596153272817 2
N	u for $\rho = 1$	
5	1.04528130312380490169235322900822 0	1.04528130056114454865633048473417 2
10	1.18770307972405209769551603844381 1	1.18770307972403400761163207500070 1
15	1.24611482730618139878266620062646 8	1.24611482730618139457160511608563 0
20	1.27888078964811472710833588167365 1	1.27888078964811472710474751084128 9

Table 30 The specific heat with size beyond our fitting data. The left column are obtained with the fitting formula (24) and the right column are obtained with BP algorithm

	Data obtained with Eq. (24)	Data obtained with BP algorithm
N	c for $\rho = 1$	
5	0.51716027467557039136185403956901 3	0.51716051160523772683560630329175 6
10	0.76811051816365598646344287152332 5	0.76811051816345374035788979548996 9
15	0.92523814901186361219951449250406 8	0.92523814901186351851682188106069 9
20	1.04130604706671911612664479135691 1	1.04130604706671911609850192737816 7
N	c for $\rho = 2$	
5	0.60888844870605630575480228703903 4	0.60888851061080028187192893611804 3

In Table 30, we present the specific heat obtained by the fitting formula Eq. (24) and the data by BP algorithm with size $N = 5, 10, 15, 20$ (Tables 31, 32).

Table 30 continued

	Data obtained with Eq. (24)	Data obtained with BP algorithm
N	c for $\rho = 2$	
10	0.867261040166647211648992207006728	0.867261040166595753683241781575513
15	1.029005211519860495847998392141416	1.029005211519860471745141018862620
20	1.148247180017501281998000470673086	1.148247180017501281990891149126682
N	c for $\rho = 4$	
5	0.656304919380385746047567881576762	0.656304950630766113382164040252364
10	0.918111415493117508675450405070246	0.918111415493092748419430447996673
15	1.082088836905833545331660660347656	1.082088836905833533497521176676883
20	1.202884869273539234743017753158652	1.202884869273539234739661228111557
N	c for $\rho = 8$	
5	0.680022822966554354733962881327128	0.680022838802143869678040316792630
10	0.943541722341561560019666980170807	0.943541722341549713987771861214547
15	1.108634803385541527903010477628312	1.108634803385541522064884456024417
20	1.230207468163357093090256751673601	1.230207468163357093088613833384342
N	c for $\rho = 16$	
5	0.691881774589583824364265101767169	0.691881783252407615668489243200063
10	0.956256875840470956659752483381501	0.956256875840468626107963408819007
15	1.121907786669434547572474050032493	1.121907786669434545704506633574112
20	1.243868767642274894557062830621890	1.243868767642274894557407464510230

Table 31 Some internal energy density for five shapes on the triangle lattice with size beyond our fitting range

	Data obtained with Eq. (29)	Data obtained with BP algorithm
N	u for triangular shape	
5	0.873604060913705583756345177664976	0.873604060898844538728806111273861
10	1.235453403254636258891683669774132	1.235453403254636260471578346986456
15	1.407395640478786519205205983127657	1.407395640478786519197891339747544
20	1.510450585232519818188153679702930	1.510450585232519818188134108705702
N	u for rectangular shape	
7	1.205391848625393400871710114437520	1.205391848617188824558185327615321
11	1.420390646436745174982557863265205	1.420390646436743604959348096055666
15	1.536706526567148993190920560852055	1.536706526567148990345243852918785
19	1.610816366206488740770278878236835	1.610816366206488740756639125527150

Table 31 continued

	Data obtained with Eq. (29)	Data obtained with BP algorithm
N	u for rhomboid shape	
5	1.05177753363249351790219569732998 6	1.05177753405834963571658137872212 0
10	1.39128069457792107759521512338046 1	1.39128069457796460835412700658705 8
15	1.53951681937164483297493919797159 4	1.53951681937164489883093342598063 0
20	1.62497760043048135448678138866569 9	1.62497760043048135475687765221614 5
N	u for trapezoid shape	
5	1.13417789066833648626353730096042 1	1.13417788987884350087959646544536 2
10	1.45516207224087213636575209182062 9	1.45516207224085937192845774774894 4
15	1.59134420540169701151302083845266 3	1.59134420540169700364620280881829 9
20	1.66885983607899283113768459150935 1	1.66885983607899283112142190878513 6
N	u for trapezoid shape	
5	1.33729447551277673933313213806194 9	1.33729447401953975207112875340304 6
10	1.60723612800973808928704527386285 1	1.60723612800972548794945440749437 3
15	1.71245999890885268457072485509960 1	1.71245999890885268062858981349028 3
20	1.77021039754673003455029324873746 5	1.77021039754673003454541480265572 0

Table 32 Some specific heat for five shapes on the triangle lattice with size beyond our fitting range

	Data obtained with Eq. (35)	Data obtained with BP algorithm
N	c for triangular shape	
5	0.33305630853203711106376871604128 9	0.33305630853012669006264177208507 7
10	0.56351268878882901000900448732433 9	0.56351268878882904282683216367730 8
15	0.71520859676419722140918774010241 8	0.71520859676419722142148047018236 0
20	0.82917324412740304981920356686557 7	0.82917324412740304981921813607509 0
N	c for rectangular shape	
7	0.54573300657412259667482057945353 5	0.54573300656175182874520452486386 3
11	0.73516326244555479709349432823393 2	0.73516326244555214665431611477696 3
15	0.86952354555475001054769171784316 8	0.86952354555475000558495605873434 7
19	0.97406756612191319868014941589470 4	0.97406756612191319865594085721931 2
N	c for rhomboid shape	
5	0.43482846897650536593529697108958 8	0.43482846951477009442990040950652 9
10	0.69809030266440339032910544465005 0	0.69809030266447547855139591982638 9
15	0.86431207200989491442654934012979 6	0.86431207200989503034257036542698 7
20	0.98683201924181327305146022348313 8	0.98683201924181327350987938465850 7

Table 32 continued

	Data obtained with Eq. (35)	Data obtained with BP algorithm
N	c for trapezoid shape	
5	0.48747616402697260877426942140994 4	0.48747616348961545242537994902404 1
10	0.76186030604234124889433451164974 3	0.76186030604233467064170596335201 0
15	0.93288476488841090646159196862878 0	0.93288476488841090505801829389651 1
20	1.05822939875838615657404892299709 9	1.05822939875838615657346588212550 2
N	c for trapezoid shape	
5	0.64546339665084746308340406967058 6	0.64546339369398397719101483237673 2
10	0.95568138874750093563109793425220 6	0.95568138874745235174875746290126 2
15	1.14132095165582049166210129551267 1	1.14132095165582047200118900802205 3
20	1.27493210059265035467226523871401 4	1.27493210059265035464827265964584 2

References

1. Privman, V., Fisher, M.E.: Universal critical amplitudes in finite-size scaling. Phys. Rev. B **30**, 322 (1984)
2. Privman, V.: Universal size dependence of the free energy of finite systems near criticality. Phys. Rev. B **38**, 9261 (1988)
3. Blöte, H.W.J., Cardy, J.L., Nightingale, M.P.: Conformal invariance, the central charge, and universal finite-size amplitudes at criticality. Phys. Rev. Lett. **56**, 742 (1986)
4. Cardy, J.L., Peschel, I.: Finite-size dependence of the free energy in two-dimensional critical systems. Nucl. Phys. B **300**, 377 (1988)
5. Onsager, L.: Crystal statistics. I. A two-dimensional model with an order–disorder transition. Phys. Rev. **65**, 117 (1944)
6. Kaufman, B.: Crystal statistics. II. Partition function evaluated by spinor analysis. Phys. Rev. **76**, 1232 (1949)
7. Newell, G.F.: Crystal statistics of a two-dimensional triangular Ising lattice. Phys. Rev. **79**, 876 (1950)
8. Ferdinand, A.E., Fisher, M.E.: Bounded and inhomogeneous Ising models. I. Speci6c-heat anomaly of a finite lattice. Phys. Rev. **185**, 832 (1969)
9. Au-Yang, H., Fisher, M.E.: Bounded and inhomogeneous Ising models. II. Specific-heat scaling function for a strip. Phys. Rev. B **11**, 3469 (1975)
10. Ivashkevich, E.V., Sh, N., Izmailian, N., Hu, C.-K.: Kroneckers double series and exact asymptotic expansions for free models of statistical mechanics on torus. J. Phys. A **35**, 5543 (2002)
11. Izmailian, NSh, Oganesyan, K.B., Hu, C.-K.: Exact finite-size corrections for the square-lattice Ising model with Brascamp–Kunz boundary conditions. Phys. Rev. E **65**, 056132 (2002)
12. Sh, N., Izmailian, K., Hu, C.-K.: Finite-size effects for the Ising model on helical tori. Phys. Rev. E **76**, 041118 (2007)
13. Salas, J.: Exact finite-size-scaling corrections to the critical two-dimensional Ising model on a torus: II. Triangular and hexagonal lattices. J. Phys. A **35**, 1833 (2002)
14. Janke, W., Kenna, R.: Finite-size scaling and corrections in the Ising model with Brascamp–Kunz boundary conditions. Phys. Rev. B **65**, 064110 (2002)
15. Sh, N., Izmailian, K., Hu, C.-K.: Exact Universal Amplitude Ratios for Two-Dimensional Ising Models and a Quantum Spin Chain. Phys. Rev. Lett. **86**, 5160 (2001)
16. Landau, D.P.: Finite-size behavior of the Ising square lattice. Phys. Rev. B **13**, 2997 (1976)
17. Stošić, B., Milošević, S., Stanley, H.E.: Exact results for the two-dimensional Ising model in a magnetic field: tests of finite-size scaling theory. Phys. Rev. B **41**, 11466 (1990)
18. Kleban, P., Vassileva, I.: Free energy of rectangular domains at criticality. J. Phys. A **24**, 3407 (1991)
19. Bondesan, R., Dubail, J., Jacobsen, J.L., Saleur, H.: Conformal boundary state for the rectangular geometry. Nucl. Phys. B **862**(FS), 553 (2012)
20. Imamura, Y., Isono, H., Matsuo, Y.: Boundary States in the Open String Channel and CFT near a Corner. Prog. Theor. Phys. **115**, 979 (2006)

21. Gaberdiel, M.R., Runkel, I.: From boundary to bulk in logarithmic CFT. J. Phys. A **41**, 075402 (2008)
22. Read, N., Saleur, H.: Associative-algebraic approach to logarithmic conformal field theories. Nucl. Phys. B **777**, 316 (2007)
23. Affleck, I.: Lecture notes, Les Houches Summer School, July 2008, vol. 89, Oxford University Press, Cary. arXiv:0809.3474 (2010)
24. Affleck, I., Ludwig, A.W.W.: The Fermi edge singularity and boundary condition changing operators. J. Phys. A **27**, 5375 (1994)
25. Calabrese, P., Cardy, J.: Entanglement and correlation functions following a local quench: a conformal field theory approach. J. Stat. Mech. P10004 (2007)
26. Dubail, J., Stéphan, J.-M.: Universal behavior of a bipartite fidelity at quantum criticality. J. Stat. Mech. L03002 (2011)
27. Stéphan, J.-M., Dubail, J.: Local quantum quenches in critical one-dimensional systems: entanglement, the Loschmidt echo, and light-cone effects. J. Stat. Mech. P08019 (2011)
28. Bauer, M., Bernard, D.: 2D growth processes: SLE and Loewner chains. Phys. Rep. **432**, 115 (2006)
29. Vernier, E., Jacobsen, J.L.: Corner free energies and boundary effects for Ising, Potts and fully packed loop models on the square and triangular lattices. J. Phys. A **45**, 045003 (2012)
30. Loh, Y.L., Carlson, E.W.: Efficient algorithm for random-bond Ising models in 2D. Phys. Rev. Lett. **97**, 227205 (2006)
31. Loh, Y.L., Carlson, E.W., Tan, M.Y.J.: Bond-propagation algorithm for thermodynamic functions in general two-dimensional Ising models. Phys. Rev. B **76**, 014404 (2007)
32. Wu, X.-T., Izmailian, NSh, Guo, W.-A.: Finite-size behavior of the critical Ising model on a rectangle with free boundaries. Phys. Rev. E **86**, 041149 (2012)
33. Wu, X.-T., Izmailian, NSh, Guo, W.-A.: Shape-dependent finite-size effect of the critical two-dimensional Ising model on a triangular lattice. Phys. Rev. E **87**, 022124 (2013)
34. Caselle, M., Hasenbusch, M., Pelissetto, A., Vicari, E.: Irrelevant operators in the two-dimensional Ising model. J. Phys. A **35**, 4861 (2002)